Assessment of the Reliability of Thermal-Hydraulic and Neutronics Parameters of Ghana Research Reactor-1 Control Systems

A thesis submitted to the:

Department of NUCLEAR ENGINEERING
SCHOOL OF NUCLEAR & ALLIED SCIENCES
UNIVERSITY OF GHANA

By

EDWARD OSCAR AMPONSAH-ABU; 10362988
BE (Kumasi), 2010

In partial fulfilment of the requirements for the award of

MASTER OF PHILOSOPHY DEGREE

In

NUCLEAR ENGINEERING

June, 2013

DECLARATION

I hereby declare that, with exception of references to other people's work which have duly been acknowledged, this work is the result of my own original research undertaken under supervision, and either in whole or in part has not been presented for any other degree at another university elsewhere.

---------- ----------

Edward Oscar Amponsah-Abu Date:

(Student)

Supervisors' declaration:

We hereby declare that the preparation and presentation of the thesis were supervised in accordance with guidelines on supervision of thesis laid down by the University of Ghana.

…… ……

Emeritus Prof. E.H.K Akaho Date:

(Principal Supervisor)

…… ……

Rev. Dr. S.Akoto-Bamford Date:

(Co-supervisor)

ABSTRACT

The thermal–hydraulics and neutronics parameters of GHARR-1 control systems were assessed for its reliability after 18 years of operation using the Micro-Computer Closed Loop System (MCCLS) and original Control Console (CC). The MCCLS and some components that control the sensitivity and the reading mechanism of the meters on the control systems have been replaced with new ones over the years, due to ageing, repairs and obsolescence. The results show that when reactor is operated at the different power levels the preset neutron fluxes at the control systems is 1.6 times the Neutron fluxes obtained using a flux monitor at the inner irradiation site two of the reactor. The average percentage of deviation of fluxes from the actual preset was 36.5% which compares very well with the reactivity decrease of 36.3% after operating the reactor at critical neutron flux of 1.0 x 109n/cm2s. The reactivity regulators were adjusted to increase the core reactivity to 4 mk and the reactor operated at 15 kW. The preset neutron flux at the control systems reduced to 1.07 times the Neutron fluxes obtained using a flux monitor at the inner irradiation site 2 of the reactor. The performance of the current micro – amplifiers in the two independent control instrumentations was assessed at an input current of 10 µA. The results showed that the flux registered on both the CC and MCCLS varied by a factor of 1.2. The correlation between neutron flux and power, as well as temperature and power at transient state produced almost the same thermal power at about 20% above the rating power of 30 kW but deviated at lower and higher power ratings. The dynamic test through positive reactivity insertion, demonstrate or confirm the inherent safety of the reactor.

DEDICATION

This work is dedicated first to the Almighty God for seeing me through the course, to Him be all the glory.

Furthermore, I dedicate this work with my deepest gratitude and love to my wife, Mrs. Dinah Amponsah-Abu, and also to my children, Mr. Foster Owusu Amponsah and Miss. Anita Yeboaa Amponsah for their enormous support, patience and prayers in bringing me this far the academic ladder.

I love you all.

ACKNOWLEDGEMENT

My sincerest gratitude goes to the Almighty God for his unending mercies and support throughout my life and in the execution of this project.

I am especially indebted to my project supervisors, Emeritus Prof. E.H.K. Akaho and Rev. Dr. S. Akoto – Bamford whose direction, criticisms and advice nurtured this work into fruition.

I also take this opportunity to express my appreciation to the Head of Department and all Lecturers of the Department of Nuclear Engineering for their support, advice and guidance throughout my stay in this University.

My sincere appreciation also goes to Dr. J. K Gbadago, Mr. Kwame Gyamfi, Mr. E.Ampomah-Amoako, Nana Ansah Adoo and Mr. M. Asamoah for their individual contributions towards the completion of this work.

My special thanks also go to all the GHARR-1 Reactor Operating Team especially Mr. Henry Obeng, whose support and corporation helped to carry out all the experiments.

My sincere appreciations also go to Mr. Isaac Baidoo, and Mr. Nicholas Opata for their time and contributions to this work.

To Prof.B.J.B Nyarko, Madam Patience Adu Serwaa, Prof. Shilo Osae, Prof.S.B. Dampare, Dr. Dickson Adomako, and Mr. Lord Yeboah, I appreciate your encouragements.

Finally to all who contributed in diverse ways, I say a big thank you and may the Almighty God Bless you.

TABLE OF CONTENTS

LIST OF FIGURES

LIST OF TABLES

ABBREVIATIONS

I & C	Instrumentation and Control
GHARR-1	Ghana Research Reactor - 1
IAEA	International Atomic Energy Agency
MNSR	Miniature Neutron Source Reactor
SLOWPOKE	Low Power Critical (K) Experiments
AECL	Atomic Energy of Canada Limited
SAR	Safety Analysis Report
CC	Control Console
MCCLS	Micro-Computer Closed Loop System
Win XP	Windows Experience
DOS	Disk Operating System
ISA	Industrial Standard Architecture
PIC	Peripheral Component Interconnect
ADC	Analog –to- Digital Converter
U-Al	Uranium –Aluminium
NiAl- NiCr	Nickel Aluminium –Nickel chromium
TECDOC	Technical Documents
AC	Alternating Current
HPG_e	High Purity Germanium

MCA	Multi-Channel Analyzer
PMT_s	Photomultiplier Tubes
NIRR -1	Nigeria Research Reactor -1
NAA	Neutron Activation analysis
DSO	Digital Storage Oscilloscope
NIST	National Institute of Standard & Technology
P_F	Neutronics Power
P_{DT}	Power due to Temperature Change

LIST OF SYMBOLS AND CONSTANTS

Symbol	Meaning	Unit
ΔT	Chang in Temperature between inlet and outlet	^{o}C
ΔE	Change in voltage between preset and current amplifier	volts
n	Neutron density	neutrons /cm^3
ρ	Reactivity	mk
C_i	Concentration of precursors at any given time	nuclei/cm^3
λ	Radioactive decay constant	s^{-1}
Φ_{th}	Thermal neutron flux	$ncm^{-2}s^{-1}$
σ_{act}	Microscopic activation cross section	m^2
N_T	Number of target atoms in the Samples	nuclei / cm^3
T	Neutron temperature	K
t_i	Duration of the exposure	sec
t_w	Delay time	sec
V_f	Volume of the core	cm^3
Σ_f	Microscopic fission cross section of the core	cm^{-1}
I	Current from micro fission chamber	μA

CHAPTER ONE

INTRODUCTION

1.1. Background

The majority of research reactors operating today were put into operation about 20 years ago, and some of them underwent modifications, upgrading and refurbishing since their construction in order to meet the requirements for higher performance. However, a few of these ageing research reactors are still operating with their original instrumentation and control systems (I&C). The I & C systems are important for reactor safety to guard against abnormal occurrences and reactor control involving startup, shutdown and power regulation.

The (I & C) systems consist of sensors that interact with the facility's physical processes to measure process variables such as temperature, water level as well as control regulation, and safety components that process the sensors' data.

The Ghana Research Reactor-1 (GHARR-1) is a Miniature Neutron Source Reactor (MNSR) with maximum thermal power of 30kW. It is classified as a low power research reactor. The general principles of design and operation are similar to other low power research reactors as SLOWPOKE 1, SLOWPOKE II. SLOWPOKE [1]. GHARR-1 was installed and attained criticality by December 17, 1994. It was commissioned on 8th March, 1995. It produces a peak or maximum thermal neutron flux of 1.0 x 10^{12}n/cm^{2}s in the core and its inner irradiation channels. The reactor is designed to be compact and safe and it is used mainly for research and development, neutron activation analysis, human resource development for non-power and nuclear power programme. Ghana's MNSR facility instrumentation is classified into the following four categories:

- Nuclear instrumentation: measures nuclear processes or reactor power, such as neutron flux density.
- Process instrumentation: measures non – nuclear processes such as reactor coolant temperature and water level.
- Radiation monitoring instrument: measures radiation, example, monitoring radiation on top of the reactor, reactor hall, reactor water purification plant and pneumatic transfer of samples and receiving room.
- Special instrumentation: encompassing all other applications, such as for measuring water conductivity etc.

In GHARR-1, two independent control systems are used to operate the reactor; control console (CC) and micro-computer closed loop system (MCCLS). Several parts and components have been replaced, as a result of ageing, upgrading and maintenance. The micro-computer control system was replaced with a new one in February, 2008 with the operating system changed from Disk Operating System (DOS) to Windows "eXPerience" (Win XP) making it user friendly. The interface board sockets have been changed from Industrial Standard Architecture (ISA) to Peripheral Component Interconnect (PCI).

The control drive mechanism was also replaced in August, 2009. Again, changes have occurred in areas like the transmitting and receiving autosyns, IC's etc. Three different sessions of beryllium plate addition of 9 mm thickness have been performed to compensate for reactivity loss due to samarium poisoning and fuel burn up. The changes have enabled the reactor to be operated up to date.

Neutron fluence and the thermal-hydraulics parameters such as the difference between the outlet and inlet temperatures of the reactor core are used to estimate the in-core power of the reactor by using a thermal-hydraulic correlation.

Measurement of neutron population in a given area per unit time (neutron flux) in the inner and outer irradiation sites can be utilised to determine linearity, repeatability and stability of the neutron measurement system, which includes detectors and secondary instruments such as the gamma dose monitoring system.

Neutron measurement in a reactor is vital for reactor control and protection because the instantaneous power of the reactor is related to the neutron population through the simultaneous release of neutrons and energy in the fission process. Instrumentation based on neutron measurement is able to determine the presence of an unwanted transient at low powers before it develops into a serious problem. Such instrumentation is also sensitive to high power transients.

As GHARR-1 is mainly used for neutron activation analysis, accurate control of the neutron flux is required. The neutron flux of GHARR-1 is monitored through a small fission ionization chamber of 5 mm in diameter. This is placed in a 10 mm diameter hole with a depth of 190 mm and is located in a beryllium reflector which is 165 mm from the center of the core.

Thermodynamic parameters of reactors include the flow rate, pressure, temperature and temperature difference, conductivity and water level. The thermal power is measured using a relationship between the reactor inlet and outlet temperature, ΔT.

Heat is generated through the nuclear fission process in the core of nuclear reactors during operation and it is cooled by natural convection and moderated with light

water. The heat is circulated or transported via the coolant system to different locations in the reactor.

Thermocouples and level gauges are used for measuring the reactor thermo-hydraulic parameters. These devices monitor the operating conditions of the reactor and provide information through the instruments mounted on the main control console and the micro-computer closed loop control systems. Measurement of the temperature difference between core inlet and outlet is accomplished by two alumel-chromel thermocouples [2]. One of them is located outside the side annular reflector near the core inlet orifice for the measurement of the inlet temperature. The other is at the upper part of the annular reflector near the core outlet orifice to measure the outlet temperature. The indicating meters of the inlet and outlet temperature of the reactor water are installed on the control console system. Voltage signals are sent to the Analog-to-Digital Converter (ADC) interface board and to the micro computer closed loop control system for display.

1.2. Problem Statement

The operation of GHARR-1 is such that there is an imputed preset flux before the reactor is started. The meters on the control systems (control console and micro-computer close loop) then adjust themselves to read the in-core flux that is generated. The GHARR-1 has been in operation for the past eighteen 18 years. Many components that control the sensitivity and the reading mechanism of the meters on the control systems have been replaced as a result of GHARR-1 ageing management policy. These changes could affect the sensitivity of these meters which could result in wrong operating parameters readings. A detailed experimental validation of the reliability of the reading of the meters has not been done for all these changes that

have occurred in the control systems. Due to the safety and high level of accuracy needed in the operation of the reactor, the control parameters that are measured by the meters on the control systems should be reliable. Reactor operation and experiments related to utilization require accurate flux and temperature. Therefore, determination of the in-core power of the reactor is dependent on the neutron fluxes and temperature registered on meters on the control systems, reliability assessment is necessary to ensure the safe operation and effective utilization of the reactor.

1.3. Research Objectives

The main objective of the research project is:

To investigate and establish the reliability of the neutronics and thermal-hydraulic parameters of the control systems via the two independent consoles of GHARR-1

The specific objectives are:

i. To study the system behaviour and response to measurements at different power levels with respect to flux and coolant temperature under steady and transient states.

ii. To study the control system response To verify the theoretical predictions of reactor power and flux parameters that result from changes in core inlet temperature and the temperature difference between the coolant inlet and outlet of GHARR-1 core at steady and transient states.

1.4. Relevance and Justification

Reliable system parameters give accurate results. Accurate instrumentation and control systems help to easily predict the reactor power for power for experimental neutronics and thermal – hydraulics.

Safety is ensured if meter readings are reliable, since the operator could differentiate between normal and abnormal situations.

This work would help to correct any discrepancies in the measurement of the reactor parameters by the two independent control systems. The results of the work would also serve as a basis for recalibration of the meters.

1.5. Scope of the research work

This work is centred on the investigation of the reliability of the neutronics and thermal hydraulics parameters of the control systems of GHARR-1 since changes have been made during the past eighteen years of its operation. Experimental investigation on GHARR-1 control systems is conducted to assess the response of meters to measurements in steady and transient conditions

1.6. Organization of the thesis

This thesis is organized into the following chapters:

Chapter one is the introduction of the thesis topic which provides adequate background information about the topic that enables the reader to understand the study. It states the nature of the problem to be investigated which will be developed further in subsequent chapters. It defines the objectives, justification and scope of the research undertaken.

Chapter two is the literature review which provides a summary of the pertinent literature with respect to what is known about this topic of study and the gaps in knowledge that must be closed. The literature review for this work includes the neutron activation method which would help to assess neutron flux density in the core at a particular preset power, reactor control systems especially of GHARR-1.

Chapter three is the methodology which describes the procedures and equipment used in sufficient details.

Chapter four contains the results of data from the study with emphasis on important observations.

The chapter five discusses the implications of the findings in relation to other relevant published studies. The Chapter also discusses the limitations of the experimental design and the achievements of the study objectives.

Chapter six gives conclusions and recommendations based on the study results.

CHAPTER 2
LITERATURE REVIEW

Introduction

The basic purpose of a reactor control system is to provide a means for starting the reactor, bringing the power output up to the desired level and maintaining it at that level, and for shutting it down in the course of routine operations. Basically, there are four general methods to vary the effective multiplication factor (or reactivity) of the reactor. These are addition or removal of Fuel, Moderator, Reflector, or Neutron absorber.

The simple and convenient way of controlling a reactor is the insertion or withdrawal of control rod (s) of a reactor core. Reactor control can be achieved through a manual control mode in which an operator uses a drive mechanism to withdraw or insert the control rod according to the requirements and indications of the measuring instruments.

Control can also be achieved through an auto mode in which the measuring instruments, control instruments, drive mechanism and control rods are connected to automatically perform the auto control of a reactor. A nuclear reactor has a protection system designed to shut the reactor down automatically in the event that potentially unsafe conditions should arise.

2.1. Description of Ghana Research Reactor-1[3]

GHARR-1 is a 30 kW tank-in-pool type research reactor. It is cooled by natural convection and can be operated at its maximum thermal power corresponding to neutron flux of $1x10^{12}$ n/cm^2.s. The reactor complex contains 5 major components.

These are the reactor assembly, control console, auxiliary systems, irradiation system and the pool containing light water. All these form the whole reactor to ensure safe operation and full utilization of the MNSR reactor.

2.1.1. Reactor Assembly:

The reactor assembly consists of the reactor vessel which contains the reactor core, beryllium (Be) reflector, small fission chambers for detecting neutron fluxes, one central cadmium (Cd) control rod and its drive mechanism, and thermocouples for measuring inlet and outlet temperatures of the coolant, figures.2.1a & 2.1b show the features and cross sectional view respectively of a reactor assembly.. The reactor vessel is a cylindrical aluminium (Al) alloy container, 0.6 m in diameter and 5.6 m high. The container, which is built in two sections, is suspended in a stainless steel-lined water pool made of reinforced concrete. Some of the constituents of the reactor assembly have been briefly discussed below.

2.1.1.1. Reactor Core:

The core consists of fuel elements, which form a fuel cage. The cage is inside an annular beryllium reflector of inner diameter 231 mm, outer diameter 435 mm, height 238.5 mm and rests on a lower beryllium reflector plate with a disc shape of 290 mm diameter and thickness of 50 mm. The top beryllium reflector is composed of group of semicircular beryllium shims with different thickness, their diameter being 243 mm. The volume of the reactor vessel is 1.5 m^3. GHAAR-1 core employs 90.2% enriched uranium-aluminum (U-Al) alloy admixed in aluminum matrix as fuel. They are arranged in 10 multi-concentric circle layers at a pitch distance of 10.95 mm. The fuel

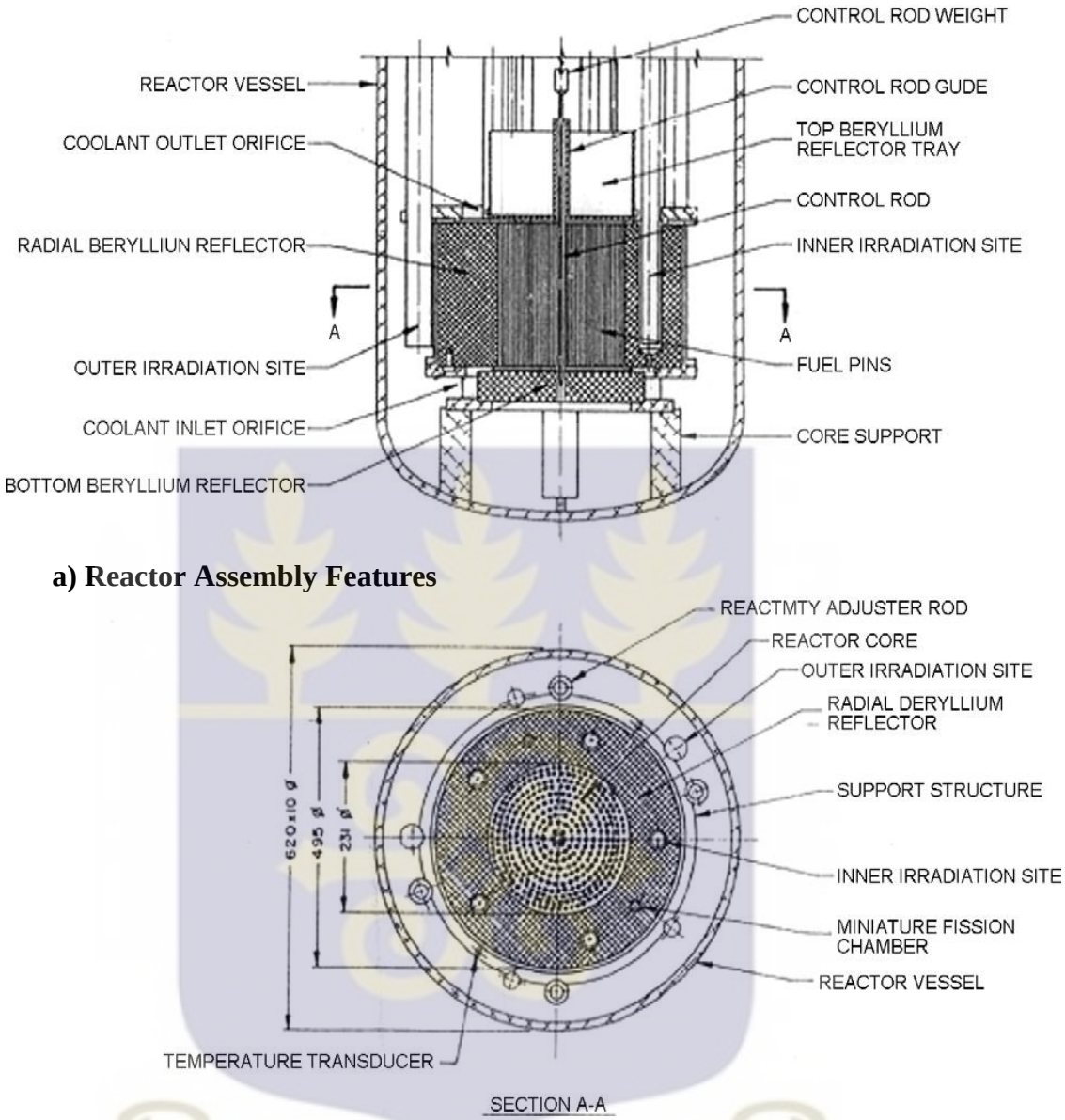

a) Reactor Assembly Features

b) Cross-Sectional View of Reactor Assembly

Fig. 2.1 Reactor Assembly

cage consists of an upper and lower grid plates, four tie rods and a guide tube for the control rod. Screws connect the two grid plates and four tie rods. The total number of lattice positions is 354 and the number of fuel elements is 344. The remaining positions are occupied with 6 dummy aluminium elements.

2.1.1.2. Irradiation Sites:

There are 5 inner irradiation tubes installed within the beryllium annulus. Five outer irradiation tubes are also installed outside the beryllium annulus.

2.1.1.3. Beryllium Reflectors:

The annulus and lower reflectors are spaced to form the lower orifice, which controls water flow through the core. The top plate of the core and annulus are spaced to form the upper orifice. An aluminium tray holds the upper reflector, which contains semicircular beryllium, shims which are added approximately once a year to compensate for fuel burn-up and samarium (Sm) poisoning.

2.1.1.4. Control Rod:

The reactor is designed to have self-limiting power excursion characteristics. Only one (1) control rod is at the centre of the reactor core. A fail-safe principle is adopted in the design of the reactor control system. A single cadmium rod is used for regulating the power level, compensating for fuel consumption, start-up and shutdown of the reactor. The control rod drive mechanism is mounted on the top plate of the container.

2.1.2. Pool Water

The pool is designed in accordance with industrial building standards. Its inside diameter is 2.7 m, depth below ground is about 6.5 m and the wall thickness is 0.4 m. The pool is made of reinforced concrete and lined with stainless steel.

2.1.3. Auxiliary Systems

The reactor incorporates several auxiliary systems. For example, two purification systems for the reactor vessel water and the pool water are used for controlling the water quality. Some of the equipment/components that are part of the auxiliary systems are discussed below.

A reactor gas purge system is employed to pump out the gas accumulated in the top space of the reactor vessel. There is a vessel water cooling system, which is used to cool the water when the temperature of the water is high. There are monitoring systems also for water temperature and dose-rate levels, radiation detection and measurements of dose-rates at the top of the reactor vessel, the working area of the reactor hall and the reactor water deionizer column.

2.1.3.1. Pneumatic Transfer System:

There are other auxiliary systems for the utilization of the reactor such as the pneumatic transfer systems. The system known as type A is suitable for medium and long time irradiation periods. Type B, a multifunction capsule transfer system can couple 4 irradiation tubes.

2.1.3.2. Multi-Channel Analyzer:

A multi-channel analyzer computer system is available for neutron activation analysis.

2.2. Basic concept of Reactor Instrumentation & Control

The Instrumentation and Control (I&C) of a nuclear research reactor is the interface between the operator and the plant figure 2.2. Nuclear reactor

instrumentation is designed so as to emphasize the reliability, redundancy and diversity of control systems.

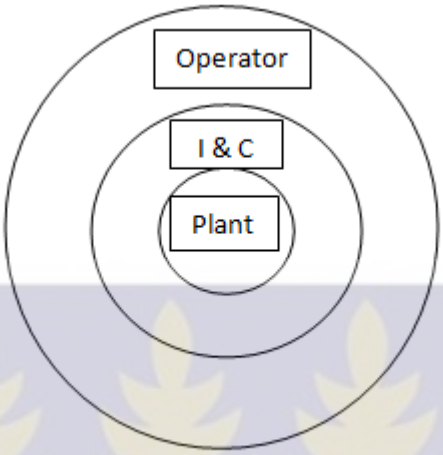

Fig.2. 2: I & C interface between the operation staff and the plant

The main functions of the I&C shell are to provide to the operating staff information about the plant, to run open-loop and close-loop control systems and to process commands from the operation staff [4]. These functions enable the operating staff to:

- Operate the plant safely and efficiently in all its operational states.
- Take measures to maintain the plant in a safe state or to bring it back into such a state after the onset of either accident conditions or design basis events.
- Supervise specific tasks.

The control instruments are used to measure and adjust neutron flux level in the reactor. Through instrumentation the reactor can be started up, shut down and operated at a stable rated power level. The function of protecting the reactor from exceeding the rated power can be achieved through the control instruments. The design of control system takes into consideration the designs of other systems. The physical design and the reactor complex design requires the consideration and the

locations of the neutron detectors, control rods with their drive mechanisms and drive mode, the worth and the speed of the control rod.

The arrangement of the control console must also incorporate the arrangement of the equipment of the control system and other systems such as dose and thermal hydraulic systems.

2.2.1. Working Principles of GHARR-1 Control Instrumentation Systems

Since the power level of a reactor is virtually proportional to the neutron flux, the obvious basis for reactor control is to vary the effective multiplication or reactivity. If the effective multiplication factor is greater than unity, the reactor is supercritical, and the power level will increase continuously. Upon decreasing the factor to unity, so that the reactor is just critical, the power output will remain constant at the level attained at the time. By making the reactor subcritical, i.e, by reducing the effective multiplication factor below unity, the power level will be decreased. Multiplication factor (k) is defined as the ratio of the number of fissions in one generation divided by the number of fissions in the preceding generation, or:

$$K = \frac{\text{Number of fission in one generation (Ni)}}{\text{Number of fission in preceding generation (Ni-1)}} \qquad 2.1$$

For a critical reactor for each neutron born, exactly one neutron must cause fission in the next generation. There are six factors that govern the production, leakage and absorption neutrons, and enable the quantitative description of the components that govern the multiplication factor in the neutron cycle.

The balance between the neutrons' production and their absorption in the core and leakage out of the core determines the value of the multiplication factor. If the

leakage is small enough to be neglected, the multiplication factor depends only upon the balance between production and absorption and is called the infinite multiplication factor, k∞ (an infinitely large core can have no leakage). When the leakage is included, the factor is called the effective multiplication factor (keff). By definition, the multiplication constants keff and k∞ are dimensionless number [5].

In the reactor, the reactor water inlet and the outlet temperatures and pool water temperature are monitored through NiCr-NiAl thermocouples. The cold ends of the thermocouples are in the room temperature state and the room temperature change is compensated by a copper – constantan bridge. The voltage signal produced by the thermocouple is in the magnitude of mV, which cannot be sampled directly by the computer. In the control interface, the voltage signals from the thermocouples are amplified 1000 times. The amplified signals are sent into the channel number zero of the Analog –to- Digital Converter circuit in the computer for display.

The circuit diagram in figure 2.3 illustrates the working principles of GHARR-1 control instruments which facilitate reactor operation. The working principles is dwell more on Neutronics and controls.

The circuits consists of amplifiers A_1, A_2 and A_3; band-change comparator, band-change control circuit, band-change transfer circuit, Digital-to-Analog (DA) converter, order of magnitude comparator, rod position comparator, flux comparator, flux control circuit, over-power protection, alarm circuit and low voltage power supply.

A_1 is the current-voltage transformer, which turns the weak current from the micro-fission ionization chamber figure 2.4 into the measurable voltage V_0. A_2 is the voltage proportional amplifier, which amplifies V_0 into V_1. V_1 is the voltage signal

corresponding to the reactor neutron flux, whose value is displayed on the digital board meter. A_3 is also a voltage comparator amplifier, which amplifies V_1 into V_1'. The value of V_1' is then sent to the band-change voltage comparator and compared with upper threshold, 6.0 V and lower threshold of 0.46 V of the comparator. When the V_1' exceeds the upper threshold or is lower than the lower threshold, the comparator will output a pulse signal to trigger the band-change control circuit to change band [6].

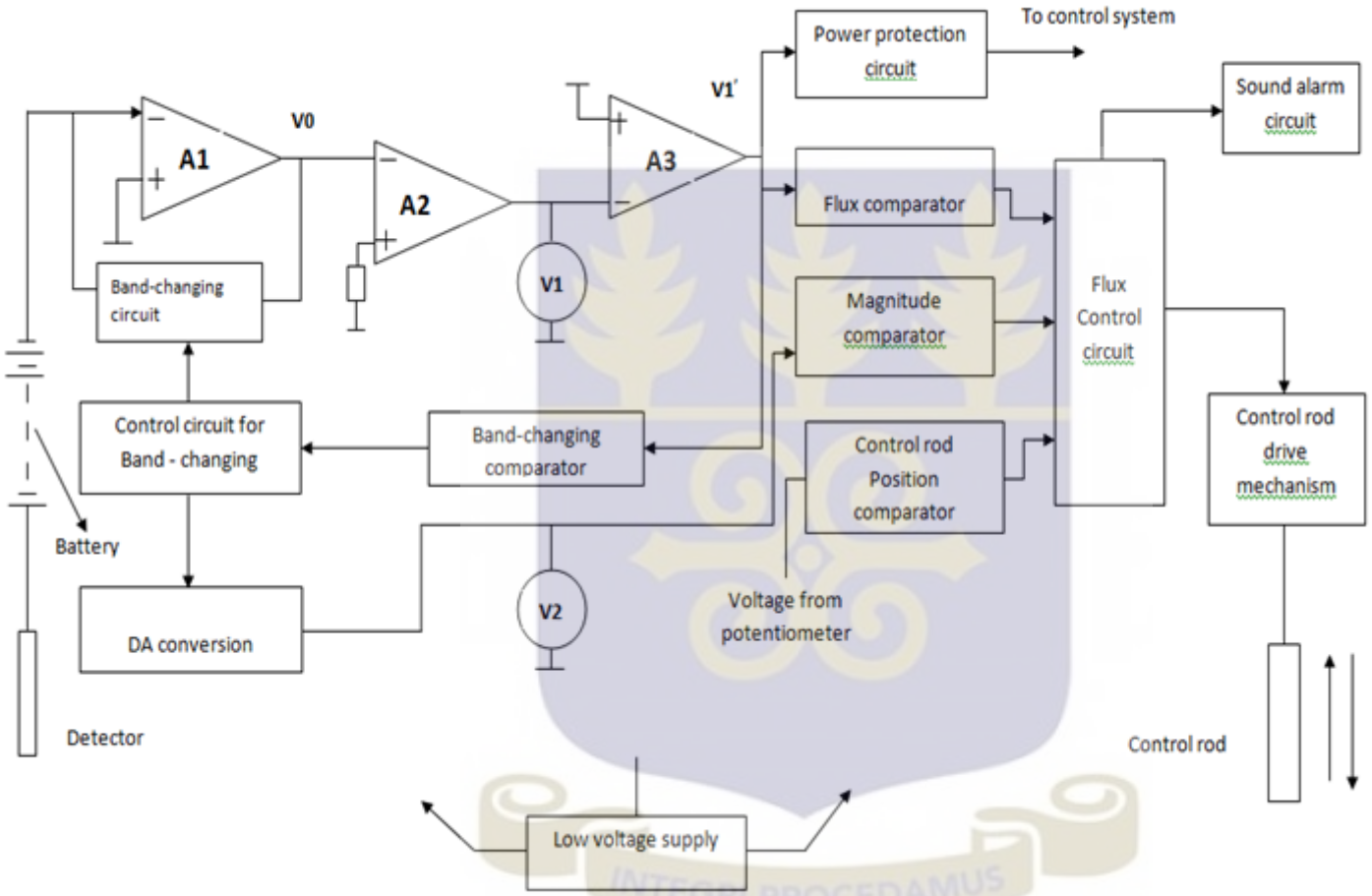

Fig.2.3 Diagram of Control Instrumentation

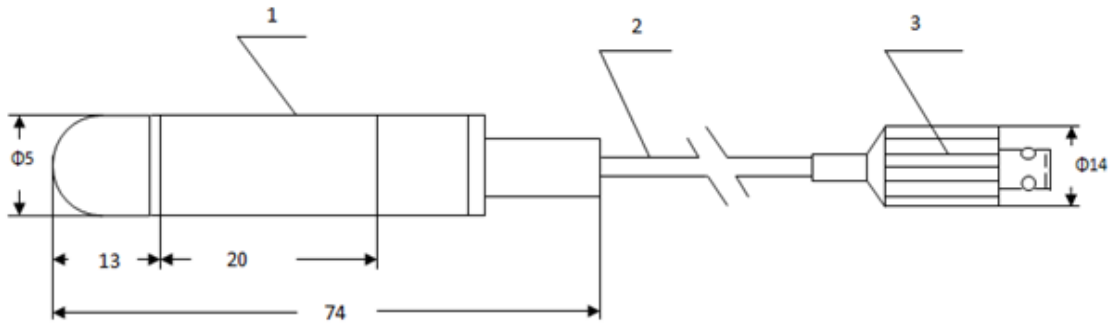

Figure 2.4 Micro fission chamber

2.2.1.1. In-core micro-fission chamber for GHARR-1

With GHARR-1, two small vertical holes of diameter 10 mm and depth 190 mm are located in the annular beryllium reflector for fission chambers. The fission chambers provide input signals to the control system and are used for the determination of thermal neutron fluxes in the inner irradiation sites at positions located 165 mm radius from the reactor core centre.

The LB1120 type micro fission chamber is an on-line gas radiation detector, which gives average transient current proportional to thermal neutron flux shown in figure. 2.4. It is used for measurement of thermal neutron flux in the core. The fission chamber has the advantages of large signals, transient response and high accuracy. Being small (Φ5x74 mm) and using integral magnesium oxide isolated nickel cover hard cable and sealed gas-filled structure, the micro fission chamber is able to operate in the environment of high temperature, high radiation field, corrosion and water soaking. It is connected with computer to realize on-line and automatic measurement of thermal neutron flux. The measuring range of a weak current

amplifier is between $10^{-9} – 10^{10}$ A. If the current is smaller than 10^{10} A, special measures are employed. The upper limit of weak current amplifier is determined by the sensitivity and position of the detector and the neutron flux to be measured. The neutron detectors are selected to match a particular neutron measuring instruments, and usually, current types of neutron detectors are employed.

The micro fission chamber composed of (1) detector, which detects the neutron flux population in the reactor core (2) connecting cable, through which current signals picked by the detector is coupled to the micro-current amplifier and (3) connector is fixed to a BNC socket at the back of the interface board, figure 2.4 [7]:

2.2.1.2. Servomotor in the control rod drive mechanism

The control rod drive mechanism is mounted on the top cover plate of the reactor vessel. It consists of a small AC servomotor Figure.2.5, an electromagnetic clutch, a gearbox, a winch drum linked with the steel rope and an autosyn figure 2.6.

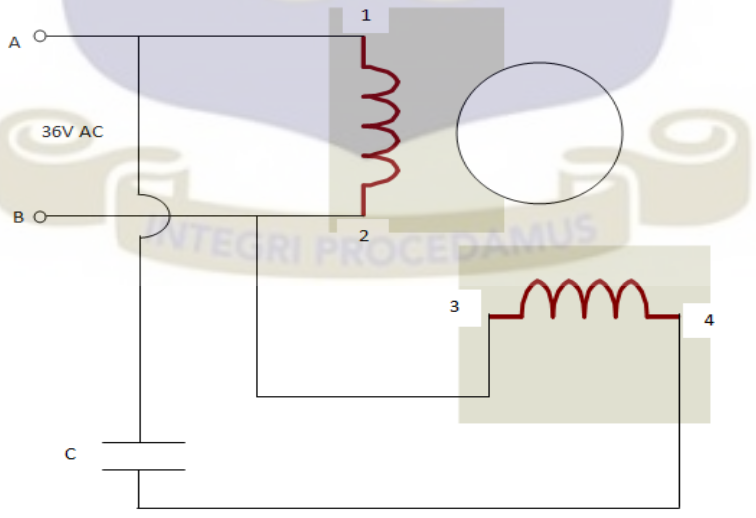

Fig. 2.5 AC Servomotor

Fig. 2.5 presents a compact AC servomotor, model SD-4SE. Its rotor is of squirrel – cage type with reduction gearing. The maximum power consumption of the motor is 10 watts, with rotary speed of 45 rpm on the main shaft.

Windings 1 & 2 are the auxiliary windings, and 3 & 4 the major windings. The motor is operated by a 36 V AC power supply. The component C is a phase – shift capacitor with a capacity of 10 µF. When end 3 of the winding 3 & 4 is connected to B as shown in the diagram, and end 4 to A through the capacitor C, the motor rotates forward or clockwise; but when end 3 is connected to A, and end 4 to B, the motor rotates in reverse direction or anti-clockwise. The main function of the motor is either to withdraw or insert the control rod in or from the reactor core [8].

2.2.1.3. Autosyn in the control system

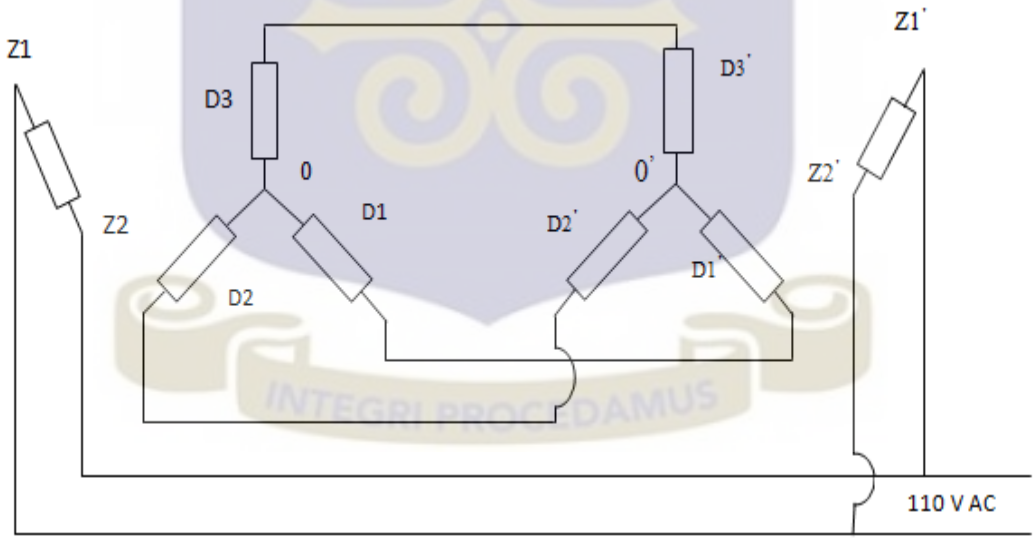

Figure 2.6 Sending and receiving autosyn

Figure. 2.6 show the diagram of a sending and receiving autosyn, an inductive motor system. Winding Z_1 Z_2 of the sending autosyn is located in the control drive mechanism whiles winding $Z'_1Z'_2$ is the receiving autosyn located in the control rod position indicator fixed in the control console. Both windings are

powered by a 110 AC Voltage simultaneously. Voltages are induced on windings D1O, D2O , D3O and D'_1O', D'_2O', $D_3'O'$. Equilibrium could only be achieved when voltages across $D_1O = D'_1O$, $D_2O = D'_2O'$, D_3O = D3O else, the autosyn rotates until equilibrium is attained [8].

2.2.1.4. Drive mechanism of control rod

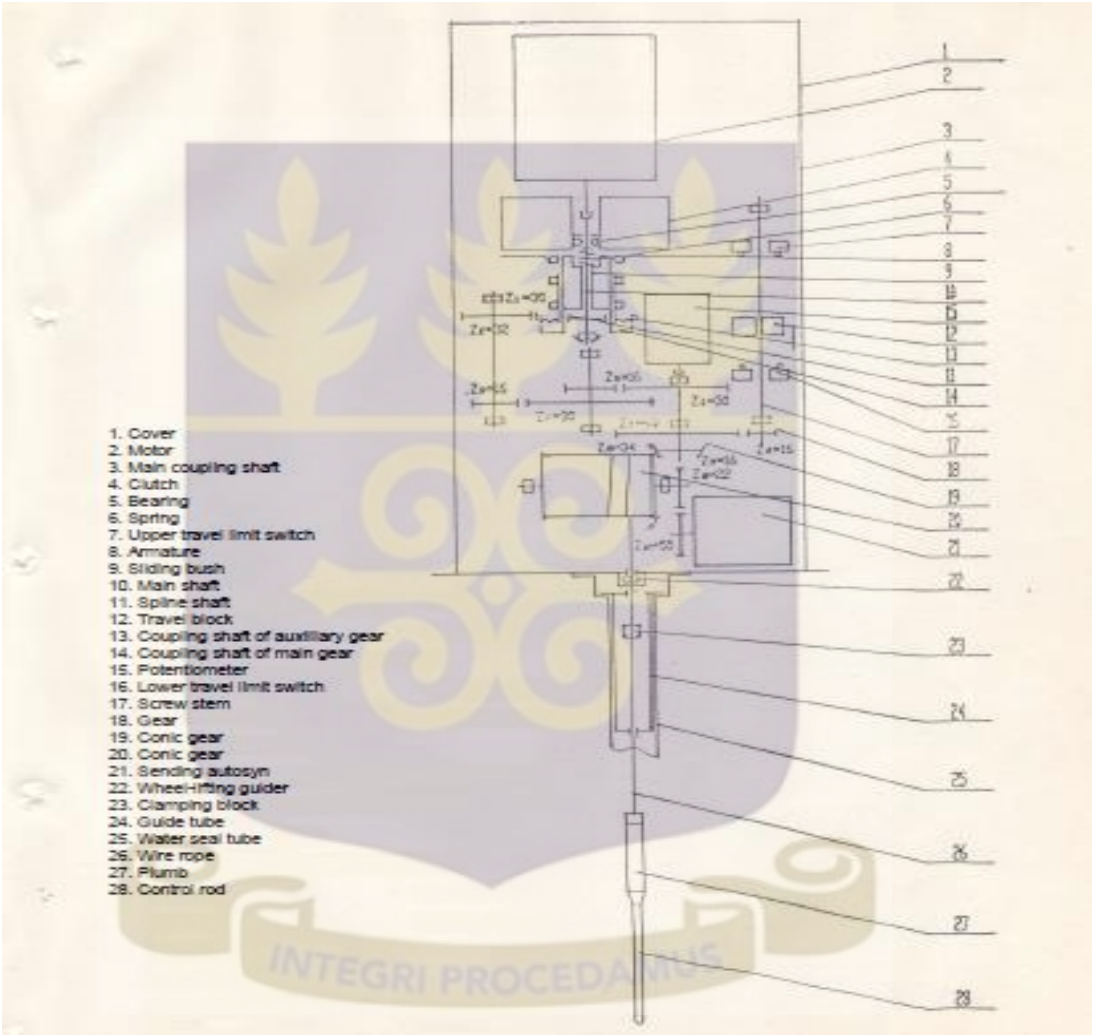

Figure 2.7 Schematic diagram of control rod drive mechanism [8]

Figure 2.7 shows the schematic diagram of the control rod drive mechanism. The servomotor and electromagnet are energized when the power is applied to the motor and the 'Protection In' button on the control console is depressed. For this case the electromagnetic clutch is closed. When receiving the signal for control rod

withdrawal or insertion, the motor will rotate clockwise or anti-clockwise; this rotation drives the gear and this operates the winch drum. The drive mechanism moves the control rod up or down at a speed of 8.7 mm/s. In case of any abnormal condition, the power supply to the clutch is cut off, the clutch immediately opens and the control rod, weighing 1 kg, will fall rapidly into the core. By so doing, fast reactor shutdown is achieved. There are limit switches provided in the control rod drive mechanism to limit movement of the control rod. The switches are connected to a circuit on the main control console, which indicates the rod position either on the top or bottom of the core through the display lights. The autosyn of the drive mechanism is connected to the rod position indicator on the main control console to show the exact position of the control rod in the core, figure. 2.7 [8].

2.2.1.5. Power regulating system of GHARR-1

A comparator circuit is used to compare the preset voltage E_o with the output voltage E of the weak current amplifier and output a difference $\Delta E = E_o - E$ to the logic circuit, Figure. 2.8. The logic circuit or power amplifier receives the signal ΔE from the comparator circuit. If ΔE is equal to zero, the motor will remain stationary; if ΔE is positive, the motor will be turning and the drive mechanism will then withdraw the control rod; on the other hand, if ΔE is negative, the motor will be turning in opposite direction and the drive mechanism will insert the control rod [8].

The central control and monitoring are required for the reactor and is performed by the control circuit and the control console. The reactor can be started up, shutdown or maintained at a certain power level or tripped by auto or manual mode.

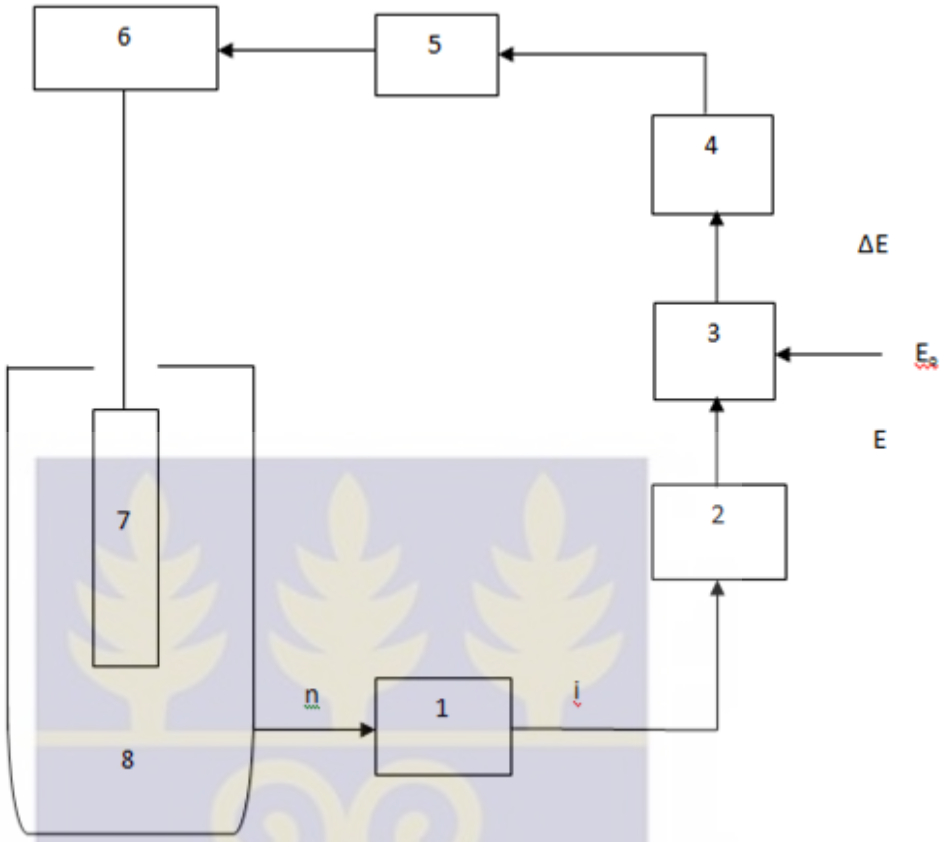

Figure. 2.8 Power regulating system of GHARR-1

1. Neutron detector
2. Weak current amplifier
3. Comparator circuit
4. Logic circuit
5. Motor
6. Drive mechanism
7. Control rod
8. Reactor vessel

2.2.1.6. Control System of GHARR-1

The layout of the main control console is presented in figure.2.9. The reactor is controlled either through the main control console or through a computerized control system shown in figures. 2.10 a and b. The control system consists of a single cadmium control rod, a neutron flux detector and a solid-state comparator control device circuit for manual or automatic control of reactor power or neutron flux. The following reactor parameters can be monitored: reactor power (neutron flux), control

rod position, gamma dose, inlet and outlet water temperatures, temperature difference, reactor and pool water conductivity.

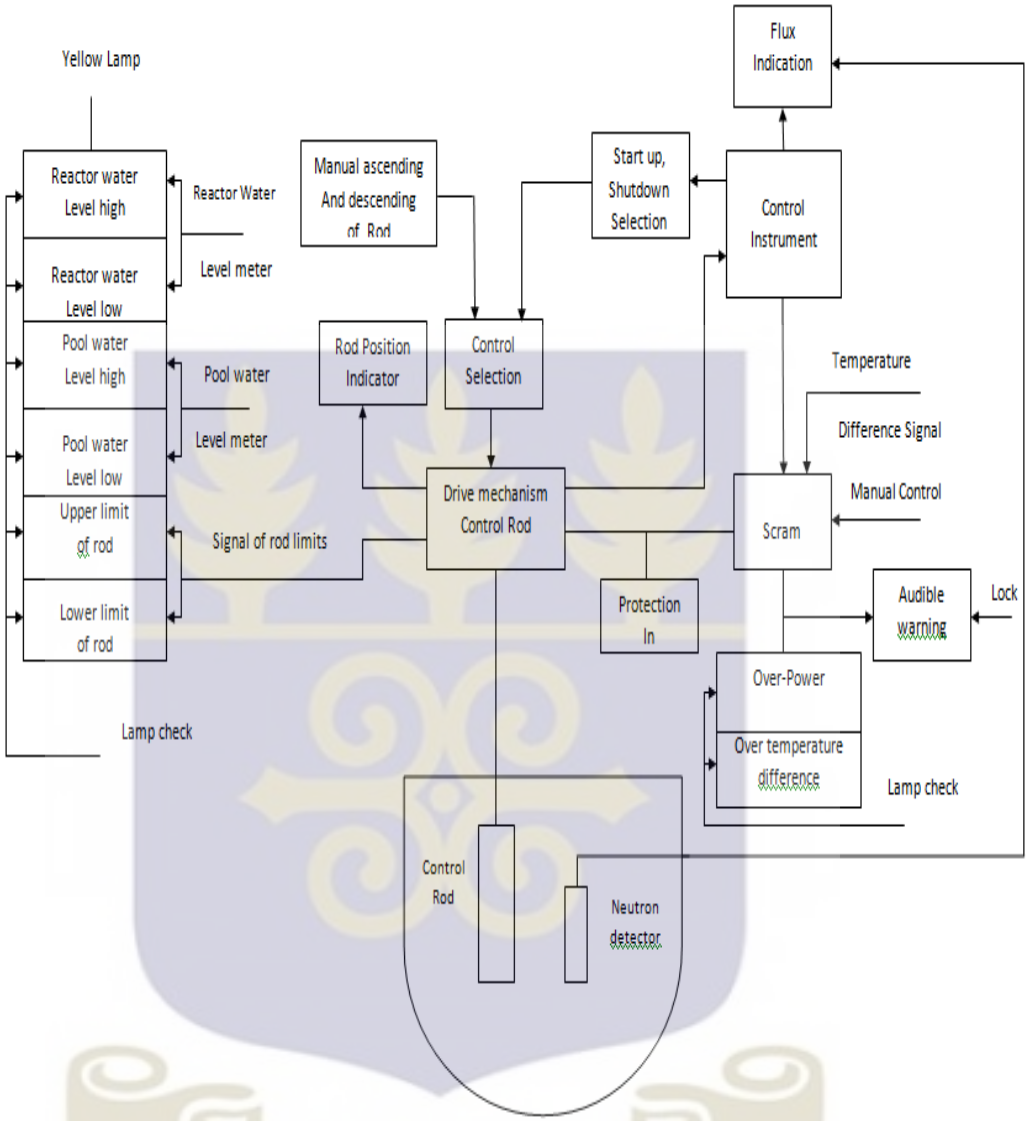

Figure. 2.9 Control Console Schematic Diagram [8]

The range of the reactor control mechanism system for automatic control covers 10^8 – 10^{12} n/cm^2.s of neutron flux. The working range for neutron activation analysis is 10^{11}-10^{12} n/cm^2.s while the range for reactor physics experiments is 10^9 – 10^{11} n/cm^2.s.

As GHARR-1 is mainly used for neutron activation analysis, accurate control of the neutron flux is required. To achieve this, the following control modes are adopted:

Figure 2.10a Micro Computer Closed Loop System

Figure.2.10 b Control Console

a) When the deviation of neutron flux from the setting value is less than + 0.5%, no regulation will be made by the system;

b) When the deviation is more than + 0.5% and less than 1.0%, fine (i.e. slow speed) regulation will be made by the control rod;

c) However, when the deviation is more than 1.0%, coarse (i.e. high speed) regulation will be made. Both quick response and accuracy of the control system are ensured so that the neutron flux can be stabilized within + 0.5% [9].

2.2.1.7. Computerized Control System

The computerized control system is designed to achieve a stable flux with accuracy of ±1.0%. The block design of this system is shown in Figure.2.11. The interface board AC6610P is in the Peripheral Component Interconnect (PCI) socket inside the computer. Most data of the MNSR are collected through Analog-to-Digital Converter (ADC) channels to the computer. Other signals are channeled through I/O input where the I/O output signals are used to control the circuits in the control box and to operate the MNSR [9]. In case the threshold of the thermal power is exceeded, power to the electric magnetic clutch in the control drive mechanism is cut off and the control rod rapidly inserted into the core by gravity. A scram push button is provided for the operator to press to shut down the reactor. When the limits of the neutron flux, temperature, gamma-dose and rod position are exceeded, alarm is given and the trips off the reactor. The position signal of the control rod in the reactor is given by a multi-turn potentiometer geared with the drive motor.

Software plays a decisive role in controlling the precision, response time, stability and safety of the control system. The control software written in Visual C^{++} [9] performs the following functions:

i. It collects and displays, in real time, various operating parameters of the reactor including neutron flux, position of the control rod, temperatures of the reactor inlet, outlet and pool water, γ-dose on the reactor top, electrical conductivity of the reactor water and pool water. Meanwhile, it computes and displays such parameters as integral neutron flux, reactivity, etc.

ii. It compares the data collected with the setting value so as to determine whether regulation needs to be made and how much it should be

iii. It detects whether motions of the central rod are in conformity with the control signals given. If there is non-conformity, the system will adjust itself to be in tune.

iv. It compares various operation parameters with their limit values and when these limits are exceeded the corresponding warning signals will be given.

v. It records operation of the reactor, including integral neutron flux, burn up and operating times. The operating log is printed out after each shutdown

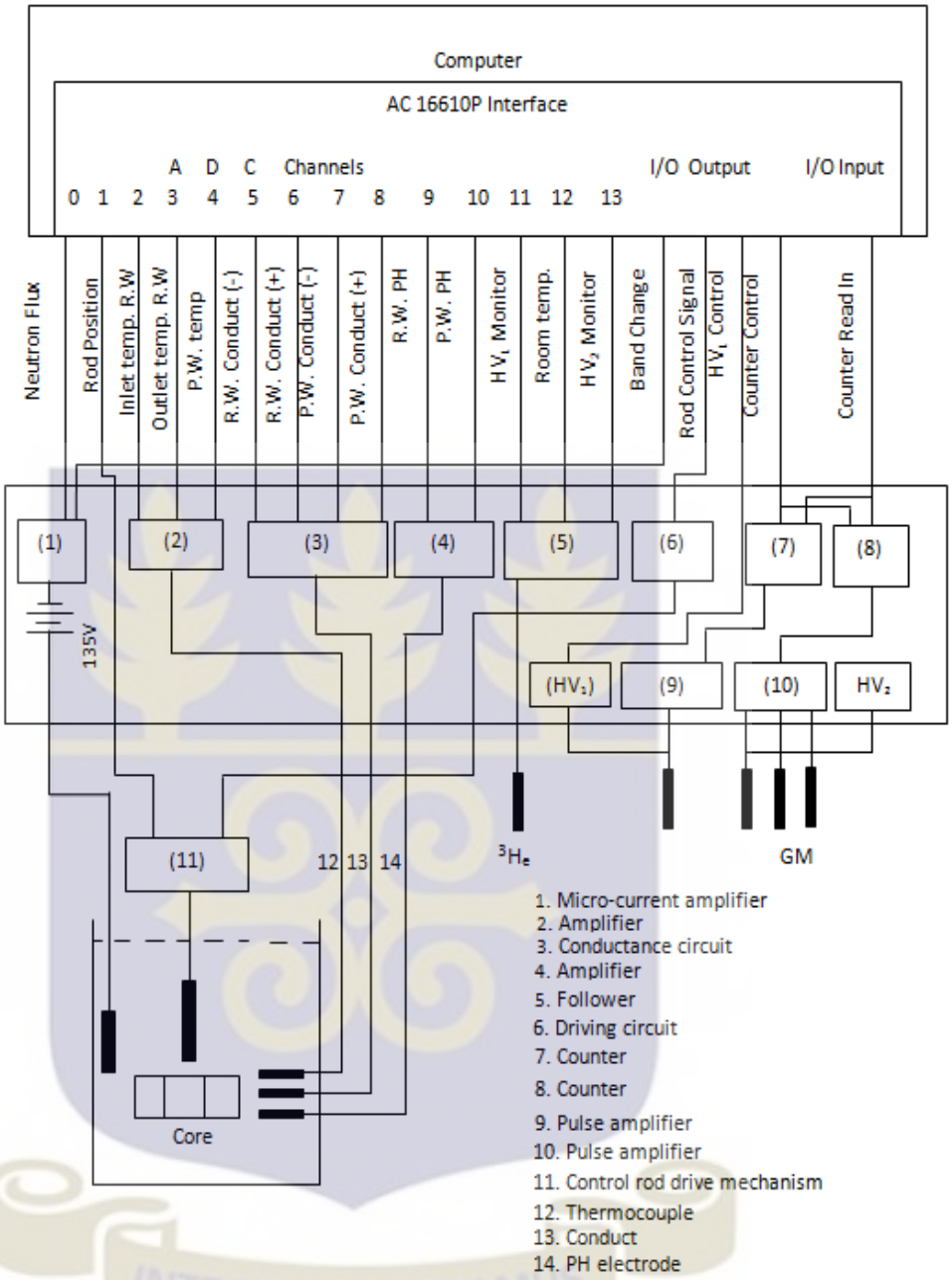

Figure.2.11. Computer control diagram

2.3. Neutron activation method

Activation analysis is an analytical method for the determination of elements and its quantity (relative concentration), based on the conversion of stable nuclei to radioactive nuclei through nuclear reactions, and measurement of the reaction products. In neutron activation analysis (NAA), the nuclear reactions occur by bombarding the material to be analyzed with neutrons.

The nuclei of certain naturally occurring isotopes can be transformed into radioactive ones by exposing the material to neutron radiation, and the activity of the radioactive products produced can be measured by means of appropriate counter system as shown in figure.2.12. In addition to the factors determined by the conditions of measurement, the activity is affected by the neutron flux at the point of irradiation and by the activation cross section of the target material which in the present case is the neutron detector. Provided the activation cross section is known, the neutron flux can be determined by measurement of the activity of the sample irradiated.

The following methods are available:

- Absolute counting technique using pure cobalt, pure gold, or cobalt-aluminum or gold-aluminum alloy.
- Standard foil technique using pure gold, or gold-aluminum alloy, and
- Secondary standard foil techniques using pure indium, indium-aluminum alloy, and dysprosium-aluminum alloy.

The techniques presented are limited to measurements at room temperatures. Special problems arise when making thermal-neutron fluence rate measurements in high temperature environments. These methods can be extended to use any material that

has the necessary nuclear and activation properties that suit the experimenter's particular situation.

The standard foil technique uses a set of foils that are as nearly identical as possible in shape and mass. The foils are fabricated from any material that activates by an n, γ reaction, preferably having a cross section approximately inversely proportional to neutron speed in the thermal energy range. Some of the foils are irradiated in a known neutron field (at National Institute of Standards & Technology - NIST or other standards laboratory). The foils are counted in a fixed geometry on a stable radiation-detecting instrument. The neutron induced reaction rate of the foils is computed from the counting data, and the ratio of the known neutron fluence rate to the computed reaction rate is determined. For any given foil, neutron energy spectrum, and counting set-up, this ratio is a constant. The four materials required for the techniques in this method are cobalt, gold, indium, and dysprosium. These metals are available commercially in very pure form (at least 99.9 %) and can be obtained in either foil or wire form. Cobalt, gold, indium, and dysprosium are also available as an alloy with aluminum, for example NIST Standard Reference Material 953. The alloy dilutions are useful for extending the range of measurement of higher neutron fluences [10] (ASTM Standards).

2.3.1. Use of activation method for calibration

After the on-site zero power and critical experiments, a steady state operational characteristics were investigated on GHARR-1, [11] using gold-foil activation method to measure the thermal neutron fluxes at three power levels: 1.5, 15 and 30 kW respectively. The values obtained were used to calibrate the measuring meter of the control console and to adjust the amplification factor for the micro-

computer control system. Calibration factor of 1.09 for the control console and amplification factor of 1.61 for the micro-computer closed loop system were obtained. In similar works, thermal, epithermal and fast neutrons were determined. In some cases, the values obtained were used to predict the power of the reactor and also for neutron characterization [12, 13].

In this work, neutron flux measurement is carried out using monitors or detectors (Au solution and Au-Al wire) to determine the thermal neutron flux in the reactor core at seven different power levels including measurement at shut down state of the reactor. The experimental samples with and without a cadmium cover of 1-mm thickness were irradiated in the isotropic neutron field of the inner irradiation site 2 of GHARR-1 facility. The induced activities in the sample were measured by gamma ray spectrometry with a high purity germanium (HPGe) detector [14].

The experimental results were compared with the measured values of the control systems and the preset neutron flux to ascertain its reliability. Reactor was operated at critical neutron flux of 1.0 x 10^9 n/cm^{2}s corresponding to 30 Watts to evaluate or assess the reactivity of the reactor core before flux measurements.

2.3.2. Gamma Spectroscopy Detectors

Radioactivity measurement of induced radionuclide in this work was performed by a PC-based γ-ray figure 2.12. It consisted of an N-type High purity Germanium detector (HpGe-coaxial type) coupled to a computer based multi-channel analyzer (MCA) via electronic modules. The relative efficiency of the detector is 40%. Its energy resolution is 1.8keV at a γ-ray energy of 1332keV of ^{60}Co. The data acquisition and identification of γ-rays of product radionuclide were identified by

their γ-ray energy (ies) via ORTEC MAESTRO-32. Determinations of the flux parameters were done by using cadmium ratio dual-monitor method. Figure 2.12 shows the gamma spectrometry set-up for the neutron flux analysis [15].

Gamma spectroscopy detectors are passive materials that wait for a gamma interaction to occur in the detector volume. The most important interaction mechanisms are the *photoelectric effect*, the *compton effect*, and *pair production*. The photoelectric effect is preferred, as it absorbs all of the energy of the incident gamma ray. Full energy absorption is also possible when a series of these interaction mechanisms take place within the detector volume. When a gamma ray undergoes a Compton interaction or pair production, and a portion of the energy escapes from the detector volume without being absorbed, the background rate in the spectrum is increased by one count. This count will appear in a channel below the channel that corresponds to the full energy of the gamma ray. Larger detector volumes reduce this effect [16].

The voltage pulse produced by the detector (or by the photomultiplier in a scintillation detector) is shaped by a multichannel analyzer (MCA). The multichannel analyzer takes the very small voltage signal produced by the detector, reshapes it into a Gaussian or trapezoidal shape, and converts that signal into a digital signal. In some systems, the analog-to-digital conversion is performed before the peak is reshaped. The analog-to-digital converter (ADC) also sorts the pulses by their height. ADCs have specific numbers of "bins" into which the pulses can be sorted; these bins represent the *channels* in the spectrum. The number of channels can be changed in most modern gamma spectroscopy systems by modifying software or hardware settings. The number of channels is typically a power of two; common values include

512, 1024, 2048, 4096, 8192, or 16384 channels. The choice of number of channels depends on the resolution of the system and the energy range being studied.

The multichannel analyzer output is sent to a computer, which stores, displays, and analyzes the data. A variety of software packages are available from several manufacturers, and generally include spectrum analysis tools such as energy calibration, peak area and net area calculation, and resolution calculation [17].

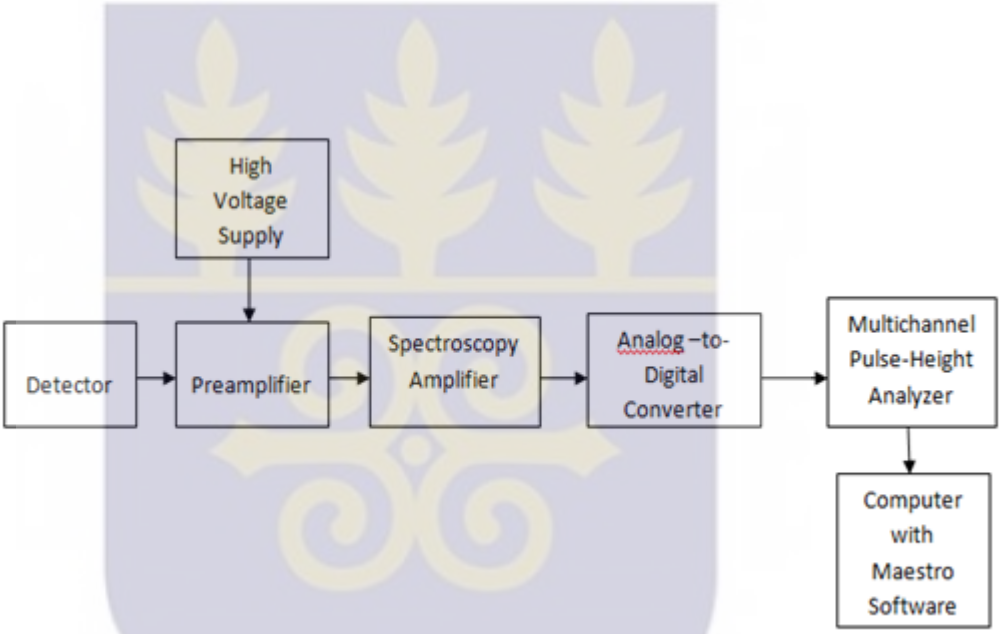

Figure. 2.12 Schematic block diagram of the gamma spectrometry used for this work

2.3.3. Determination of Thermal Neutron Flux

A gold foil of known thickness was irradiated in two different reactors Pakistan Miniature Neutron Source (P-MNSR) and GHARR-1 under similar conditions. For the effects of self-shielding, flux sink and flux perturbation which comes as a result of exposing a detector foil to thermal neutron flux, the following relationship was used for the required modifications [18, 19]:

$$\Phi = \frac{A_o(1 - F_c / R_{Au})}{N_m g \sigma_o (1 - 1/R_{1/v}) G_t} \quad - \quad (2.1)$$

Where the activity $A_o = N_m \sigma n v_o$ (dps), N_m is the number of total nucleons of detecting foil, σ is the effective capture cross-section (barns), σ_o is the activation cross-section of neutrons in 2200 m/s (barns), n is the neutron density of all neutrons affecting activation of the detector (ncm^{-3}), v_o is the neutron speed (cm/s), R_{au} is cadmium ratio of gold detecting foil, $R_{1/v}$ is cadmium ratio of detecting foil, Fc is cadmium correction for the attenuation of the fast neutrons, G_t is the thermal self-shielding factor of detecting foil, and g is the modification factor for thermal region cross-section deviation of the detecting foil from 1/v.

The activity, A_m, which is measured after decay (cooling) for period tw, is related to the activity at the end of the irradiation, A_o, in the form,

$$A_o = \frac{A_m \ell^{\lambda t_w} \lambda t}{(1 - \ell^{-\lambda t_i})(1 - \ell^{-\lambda t_m})} \quad - \quad (2.2)$$

Where λ is the decay constant of foil ($\lambda = 0.693/T_{1/2}$; where $T_{1/2}$ is the half life of the radionuclide) (s^{-1}), t_w is waiting time from the end of irradiation to the start of measurement (decay or cooling) (s) and t_i is the irradiation time (s).

This current study seeks to assess the reliability of neutronics and thermal hydraulics parameters of the control system of GHARR-1 facility. Gold solution was pipette into cotton in avoidance of self-shielding, flux perturbation and flux sink. The equivalent 2200 m/s thermal fluence rate in which a solution sample of gold has been irradiated was calculated as follows [20,21,22]:

$$\Phi_0 = \frac{R_s}{g\sigma_0} \quad - \quad (2.3)$$

where: R_s = reaction rate per target atom,

σ_0 = 2200 m/s cross section.

The reaction rate is given by

$$R_s = \frac{C\exp(\lambda t_w)}{(\in N_0(1-\exp(-\lambda t_i)))} \quad - \quad (2.4)$$

where:

C = net counting rate of the sample (flux monitor) at the time of measurement, corrected for background radiations and delay time,

λ = decay constant of 2.97 x 10^{-6} s^{-1} corresponding to the half-life of ^{197}Au of 2.7 days

N_0 = original number of atoms of nuclide to be activated (given by the product of the weight in grams of ^{197}Au in the sample (monitor) and Avogadro's number divided by the atomic weight, of the element in g),

ϵ = efficiency of the detector for specific gamma radiation at a specific counting geometry,

t_i = duration of the exposure, and

t_w = elapsed time from the end of the exposure period to the time counting (Delay time).

Since the gold sample is activated in neutron spectrum that is not totally thermalized, then the reaction rate must be corrected for epithermal neutron activation. This is

done by irradiating a similar gold solution sample shielded by cadmium of 1 mm thickness using the following equation:

$$\varphi_{th} = \frac{1}{G_{th}\sigma_o}(R_S - \frac{R_{e,cd}}{F_{cd}}) \qquad (2.5)$$

When the exposure time is small compared to the 2.7 days half-life of ^{197}Au, as is usually the case, Eqn 2.3 becomes

$$\phi_0 = C \exp \lambda t_w / \lambda t_i N_0 \sigma_0 \in \qquad (2.6)$$

The fluence during the irradiation period is

$$\Phi = \phi_0 t_i = C \exp \lambda t_w / \lambda N_0 \sigma_0 \in \qquad (2.7)$$

If the gold sample has been activated in a neutron spectrum that is not totally thermalized, then the reaction rate must be corrected for epithermal neutron activation. This is done by irradiating a similar gold sample shielded by cadmium (1 mm) thick and using Eqn 2.8 which takes into account both thermal self-shielding factor G_{th}, and epithermal self-shielding factor G_{res}:

$$\phi_0 g\sigma_0 = \frac{(R_s)_0}{G_{th}} = \frac{1}{G_{th}}\left[R_s - R_{s,Cd}\left(1 + \frac{g\sigma_0}{G_{res}I_0} f_1 + \frac{\sigma_0 w'}{G_{res}I_0}\right)\right] \qquad (2.8)$$

These yields

$$\Phi = \frac{1}{G_{th}}\left(C_B - C_{cd}\left(1 + \frac{g\sigma_0 f_1}{G_{res}I_0} + \frac{\sigma_0 w'}{G_{res}I_0}\right)\right).\exp(\lambda t_w)/\lambda N_0 g\sigma_0 \in \qquad (2.9)$$

Where C_B and C_{cd} are the ^{197}Au counting rates in the bare and cadmium-covered sample, respectively. If the sample has a negligible weight, no self-shielding correction factor is needed.

Flux at shut down state of the reactor was determined to ascertain the photo neutrons from the interactions of gamma rays through the (γ,n) reaction that provides a useful start-up source once the core is activated. There is always a residual power after shut-down which have to be investigated to assess the actual power through the neutron fluxes measured by the two control systems.

Due to ageing, modifications, refurbishments, obsolescence and repairs of some parts and components of the reactor control system, the reactor will be operated at maximum thermal flux of 1.0 x 10^{12} n/cm^2s to assess the response of the control system. The inherent safety system of the control and instrumentation would be investigated.

The assessment would justify the use of the control systems for the fuel conversion programme for GHARR-1 core.

2.4. Measurements of thermal hydraulic parameters of MNSR

The removal of heat from the core is achieved by natural convection and water recirculation. The coolant flow is at the transitional state from laminar to turbulent. The characteristic of the circulation was ascertained by computer code and thermal hydraulics simulation test [23, 24]. Safety experiments shows that for thermal hydraulics design to yield the desired rise in temperature (maintaining inherent safety) the height of inlet orifice for must remain at 6 mm and that of the outlet at 7 mm. These design considerations were used to establish the relationship

between coolant temperature and reactor power on one hand and neutron flux and coolant temperature on the other for the Nigeria Research Reactor-1 (NIRR) [25].

The semi-empirical relation amongst core inlet temperature, coolant temperature rise and power levels as obtained from simulation experiments on MNSR is expressed in the form:

$$\Delta T = (5.725 + 147.6H^{-2.64})T_i^{-0.35}P^{(0.59+0.0019T_i)} \quad (2.10)$$

Where ΔT = Temperature difference between inlet and outlet orifices (^oC)

H = Height of the inlet orifice (mm)

T_i = Inlet temperature (^oC)

The designed inlet orifice height, H, of NIRR-1 was made to be 6 mm for safety and technical reasons [25]. Therefore, substituting the value of H into Eqn. (2.10) reduces the equation to:

$$\Delta T = 7.04T_i^{-0.35}P^{(0.59+0.0019T_i)} \quad (2.11)$$

From equation (2.11), the power P becomes:

$$P = Exp\left[In\left(\frac{\Delta T}{7.04T_i^{-0.35}} \right)(0.59 + 0.0019T_i)^{-1} \right] \quad (2.12)$$

With the experimental procedures, the Nigerian Research Reactor-1 was operated at a preset flux value of 5.0 x 10^{11} n/cm^{2}s for an hour taking readings at every 10 min intervals. The flux was again preset at its licensed full-power value of 1.0 x10^{12} n/cm^{2}s to enable the investigation of power and thermal hydraulics behaviour under

this condition, as well as to determine the time that would take the control rod to reach its upper limit. The reactor was operated; neutronics and thermal-hydraulic parameters recorded after every 20 min until the reactor automatically began to shut itself down after 5 hours of operation. Similarly, GHARR-1 was operated at its nominal power continuously for 6.5 hours before the control rod attained its uppermost level of 230 mm.

The predicted power after an hour of operation at half-power for NIRR-1 was 17.43 kW with inlet temperature 28.9 ^{o}C and temperature difference ΔT 13.7 ^{o}C. The predicted power for 5hr of operation at full power was 33.45 kW with inlet temperature of 37.7 ^{o}C and ΔT 19.5 ^{o}C. The work was to investigate the behavior of NIRR-1 and the reliability of the Eqn. (2.12) in predicting the reactor power [25].

The work did not consider the reliability of the measuring devices in the control system for thermal hydraulic parameters likewise the neutronics parameters.

2.4.1. Temperature Measuring Instrument

There are three main families of temperature sensors: thermocouples, resistance thermometers and thermistors. Some old reactors still have bimetallic thermometers (binary or with local readings), but a replacement was suggested in order to allow the operator to follow closer any temperature transient from the control room.

Other temperature sensors, like semi-conductor thermometers, consisting of doped germanium sensors, have a complex resistance temperature relationship and are useful only for very low temperature measurements.

2.4.2. Thermocouples

Thermocouples can be classified into two main types: noble metal and base metal. Noble metal thermocouples, like platinum and platinum-rhodium, are used for high temperature measurements, usually in the range of 600 to 1600 °C. They are chemically inert and highly suitable in oxidizing atmospheres, however, it is important to notice that platinum and rhodium are very sensitive to gamma and neutron radiation, they are the recommended materials for Self Powered Detectors. Base metals, like chromel and alumel are used for temperature measurements in the range of 130 to 1100 °C. Although they do not show the same linearity as noble metal thermocouples, and they have higher sensitivity as compared to noble metal thermocouples, they need less sophisticated electronics. Studies have shown that chromel-alumel thermocouples are most suitable for applications close to the reactor core, where the gamma and neutron fluxes are very high. When the sensors must cover a temperature range of as high as 1000 °C it is recommended to use nicrosil-nisil type thermocouples that have become popular in the field of high temperature measurements. Usually they respond faster to temperature transients than other thermometers, and should be considered when sensor response time is an important parameter to safety [4].

2.4.3. Resistance Thermometers

Resistance thermometers, which usually employ platinum elements, have very high sensitivity, linearity and precision. They can be used safely up to temperatures of 500 °C, however, one should consider that they are sensitive to neutron and gamma

radiation, and in general they have larger time constant than thermocouples, so this must be taken into account when they are employed in the reactor protection system [4].

2.4.4. Thermistors

Thermistors are opposite to resistance thermometers. They have positive resistance coefficient (resistance increase with temperature). Thermistors have negative resistance coefficient. Thermistors have much higher sensitivities as compared to platinum resistance elements. They need simple processing electronics, which results in higher system reliability. Because of their small size, they also have smaller time constant than thermocouples, however, since they are highly non-linear sensors and because their susceptibility to radiation damage, as well as ageing, they are not recommended for applications in safety systems [4].

2.4.5. The Thermal Instruments used in GHARR-1 Research Reactor

The thermal instruments used in GHARR-1 research reactor are thermocouples and their corresponding instruments. The temperature sensors are installed at the inlet and outlet pipes of the reactor coolant and in the reactor pool which are used to measure the temperatures at these places. The temperature difference between core inlet and outlet temperatures is measured with 2 alumel-chromel thermocouples. One of them is located outside the side annular reflector near the core inlet orifice for the measurement of the inlet temperature. The other is at the upper part of the annular reflector near the core outlet orifice to measure the outlet temperature as shown in figure.8. GHARR-1 uses both chromel-alumel thermocouples and resistance thermometers for temperature measurements. The

chromel-alumel thermocouples are most suitable for applications close to the reactor core, where the gamma and neutron fluxes are very high while as, the resistance thermometers are sensitive to neutron and gamma radiation [26].

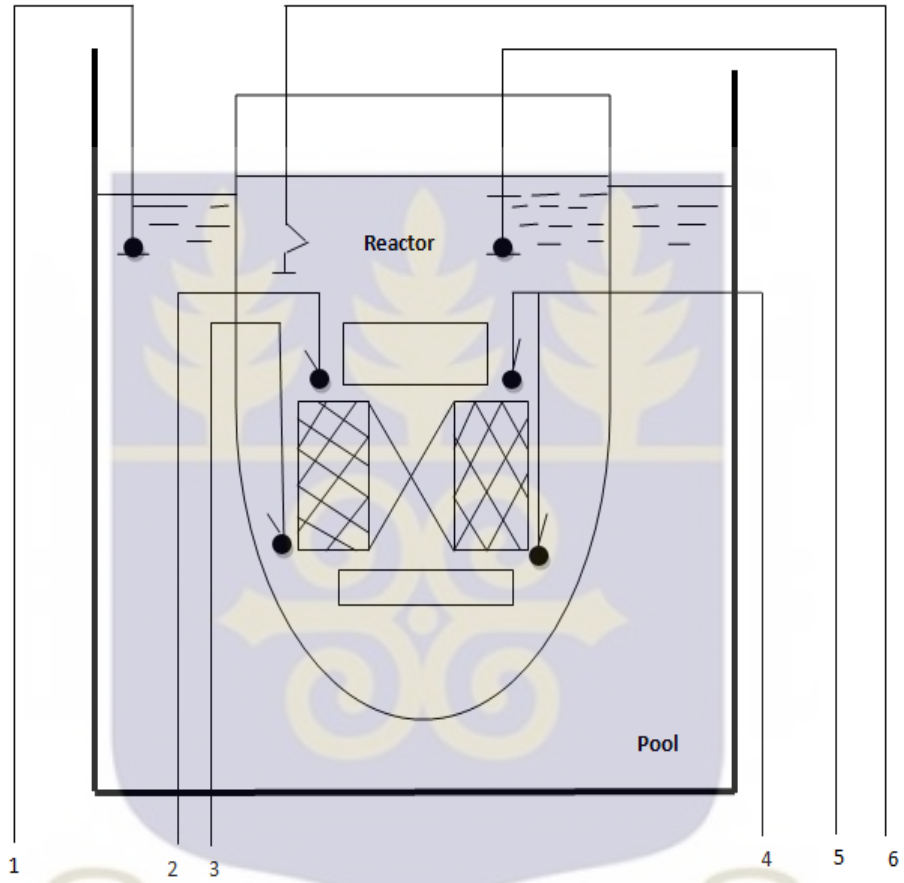

Figure.2.13. Reactor Complex Thermal-Hydraulics Monitoring System

1. Level Guage for the pool water
2. Sheathed thermocouple for outlet temp.
3. Sheathed thermocouple for inlet temp.
4. Thermoelectric junction of two pair of Chromel - alumel thimble sheathed thermocouple
5. Magnetic float level gauge
6. Thimble sheathed platinum thermal resistance thermometer for inlet temp.

Changes in core inlet temperature (T_{in}) and the temperature difference between the coolant inlet and outlet (ΔT) for MNSR were conducted in previous works but readings, especially, (ΔT) was not compared to determine the state of the temperature probes as a result of ageing and its effect on power calculations. This work will trace changes in value of the (ΔT) from 1999 to date to assess the reliability of the control system of GHARR-1.

2.5. Heat transfer (thermal–hydraulics)

The core region of GHARR-1 is located 4.7 m under water close to the bottom of a watertight reactor vessel. The quantity of water is 1.5 m^3 in the vessel, which serves the purpose of radiation shielding, moderation and as primary heat transfer medium. In addition, heat can be extracted from the water in the vessel by means of a water-cooling coil located near the top of the vessel. The water-filled reactor vessel is in turn immersed in a water-filled pool of 30 m^3.

Cold water is drawn through the inlet orifice by natural convection. The water flows past the hot fuel elements and comes out through the core outlet orifice. The hot water rises to mix with the large volume of water in the reactor vessel and to the cooling coil. Heat passes through the walls of the container to the pool water. The core inlet flow orifice impedes the natural circulation of water through the core [27, 28, 29]. A diagrammatic representation of the heat transfer mechanism is represented in figure. 2.14.

Its area is fixed during assembly of the reactor and it is deliberately chosen such that the highest power achieved during the design basis self-limiting power excursion can cause no damage to the core or present any hazard to staff about the reactor.

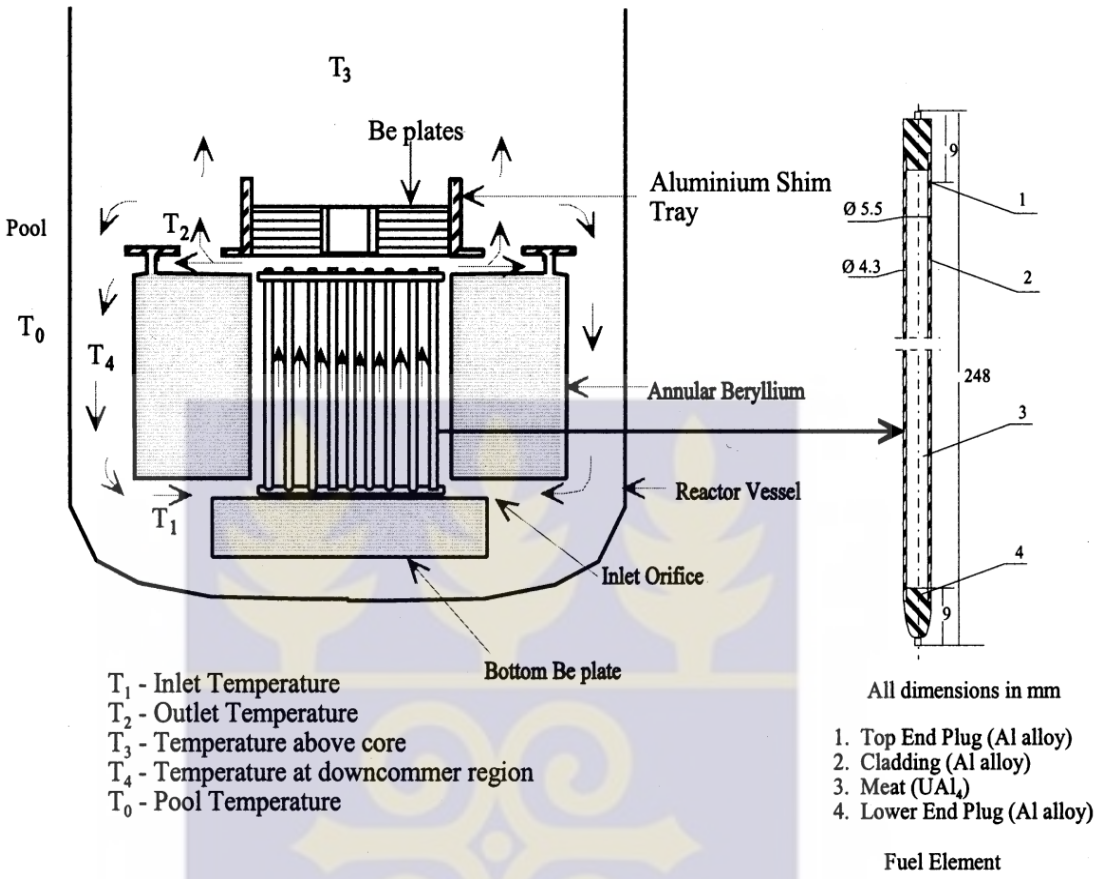

Fig. 2.14. Schematic diagram of the coolant flow pattern

2.6. Correlation between reactor neutronics and thermal hydraulics parameters

Safety experiments show that for the thermal hydraulics design to yield the desired rise in temperature (maintaining inherent safety) the height of the inlet orifice for MNSR must remain at 6 mm and that of the outlet at 7 mm. These design considerations were used to establish the relationship between coolant temperature and reactor power on one hand and neutron flux and coolant temperature on the other.

Some data generated from a graph of a "Dynamic experiments performed to investigate the effects of insertions of step and ramp reactivities on Ghana Research Reactor-1 would also be used to validate the correlation [30]. It will help to assess the reliability of the reactor neutronics and the thermal hydraulic parameters.

2.7. Safety performance of GHARR-1

The safety performance of GHARR-1 was demonstrated by releasing two types of reactivities to examine the rising, drifting and damping of the reactor power in order to access its self-regulating capability [30, 31].

In the first experiment, two cadmium (Cd) in capsules with total reactivity worth of 2.1 mk were first pumped into two inner irradiation sites of the reactor. The reactor was started and its central rod was raised until the reactor attained critical. The initial condition of the flux was 5.0 x 10^9 n/cm^{2}s and inlet temperature was 29 ^{o}C, when the critical rod position was 151 mm. The prevailing core condition was maintained for some time and the two Cd in capsules were suddenly pumped out almost at the same time. The variation of inlet temperature and temperature difference, with time were monitored on the control console and the micro-computer control systems.

The second experiment involved the introduction of a quasi-linear reactivity into the reactor. For an initial reactor condition of 1.0 x 10^9 n/cm^{2}s, inlet temperature of 29.1 ^{o}C and temperature difference, ΔT = 0.1 ^{o}C, the critical position of the control rod was 102 mm and excess reactivity was 4 mk. Under the condition of reactor shutdown, such as cold state, the control rod was withdrawn from the bottom of 0.0 mm to the upper limit of 230 mm.

The step total reactivity of 2.1 mk released generated a peak power of 37.5 kW which was attained after 7 min. 38s. The maximum temperature difference associated with the release was 21^{o}C. The release of the quasi-linear reactivity of 4 mk produced a peak power of 100.2 kW, which occurred after 4min. 3s. The maximum temperature difference between the inlet and outlet reactor water temperature was 39.4 ^{o}C.

The simulation experiments for full withdrawal of control rod after operating the reactor at 10 kW and 30 kW for half an hour before the release of the reactivities have produced the peak powers of 91.8 and 76.5 kW respectively.

The correlations in Eqns. (2.10) and (2.12) were used to predict the reactor powers at various conditions. The experiment was conducted to test the control systems in case of any failure during normal operation which could cause the control rod to be fully withdrawn. The experiments clearly demonstrated the safety of the self-limiting power excursion behavior of GHARR-1 reactor following a large and rapid increase in system reactivity.

The behaviour of the control systems were assessed in terms of transient or power excursion, but the reliability of the measuring instruments in the control systems was not assessed or investigated. This work would determine the neutron flux density in the inner irradiation sites of the core and compare to what is measured by the control systems to assess their reliability.

An auxiliary instruments, digital multimeter (MASTECH-345) interface with a

computer was used to measure the temperatures parallel to the thermocouples in the reactor (inlet, outlet and the pool temperatures). Some of the reactor water was

drained and measure directly with a thermometer and the MASTECH-345 interfaced with a computer and compare the data with the control system readings.

CHAPTER 3

MATERIALS AND METHODS

The neutronics and thermal-hydraulic parameters to be measured are: the neutron fluxes at the inner irradiation site 2 of the reactor core where maximum fluxes are measured. Reactor would be operated at different power levels taking readings of the inlet temperature, outlet temperature and the temperature difference across the core Gold solution and gold-aluminium wire would be used as flux monitor using neutron activation technique at seven (7) different power levels. Neutron flux values would be taken from the meters of the two control systems (CC and MCCLS).

Materials and methods used in the experiments conducted in the research are presented in this chapter.

3.1. Equipment and materials

Equipment and materials used for the experiment include:

1. Mastech Digital Multimeter (MAS -345)
2. (High-Purity Germanium) Coaxial Photon Detector System and Pulse Counter Apparatus
3. Systron Donner 100A Pulse Generator
4. CS-2100 100MHZ 4-Channel Oscilloscope
5. Keithley Model 263 Calibrator / Source
6. Acculab ATL-124 Analytical Scale

7. Miniature Neutron Source Reactor (Ghana Research Reactor -1)

8. Pneumatic Rabbit System for Sample delivery

3.1.1. Mastech Digital Multimeter [32]

Mastech Digital Multimeter (MAS-345) is an auto ranging professional measuring instrument. The meter has been designed according to IEC-1010 concerning electronic measuring instruments with an overvoltage category (CAT II) and pollution II. Digital reading is 3999 counts and the bar graph consists of 38 segments for LCD, capable of performing the functions stated below:

The meter consists of "K" type thermocouple (chrome –alumel) and RS232C serial interface cable exclusively designed for interfacing the meter with a PC (Optional). The meter has a temperature range of 0oC to 400oC at 1oC resolution with accuracy of ±3.0%. The instrument was used to measure the inlet temperature of the reactor coolant.

- DC voltage measuring (Auto Ranging)

- AC voltage measuring (Auto Ranging)

- DC current measuring

- AC current measuring

- Temperature measuring

- Resistance measuring (Auto Ranging)

- Capacitance measuring

- Diode testing

- Transistor testing and

- Audible continuity testing

3.1.2. Coaxial Photon Detector System and pulse Counter Apparatus [33]

The main components of the detector unit, which is an *n*-type High Purity Germanium (HPGe) detector, include a solid- state photon detector immersed in liquid Nitrogen and DSPEC jr 2.0 a unique ORTEC Detector Interface Module (DIM).

The detector is a vertical cryostat mounted with a diameter of 63.0 mm and a length 65.0 mm with end cap of 4 mm. The detector model number is GMX40P4 of a POP TOP cryostat configuration.

The DSPEC jr 2.0 is an integrated gamma spectrometer based on digital signal processing. It has a 240 x 160-pixel LCD display for viewing presets, like the high voltage settings and status, stabilizer settings, SMART-1 detector status, and shutdown mode. The DIM is designed to supply bias close to the detector so that the cable carries only signal and low-voltage power. The system runs on 8K ORTEC MAESTRO-32 MCA Emulation Software. The interface module is connected to the PC through a USB Port.

The detector operates at a bias voltage of – 4800 V, and has a resolution of 1.95 keV (FWHM) at 1.33 MeV, ^{60}Co. The detector has a relative efficiency of 40 %.

By means of the MCA card, the spectra intensities are accumulated for a reset time. In order to minimize electronic noise created by thermal excitation of electrons from valence to conduction bands, liquid nitrogen of temperature of -196 ^{o}C is used.

The high – purity germanium, coaxial photon detector system with its pulse counter apparatus was used to help correlate the energies released by the flux monitor (^{197}Au) after irradiation and determine the net area of the peak generated.

3.1.3. Systron donner model 100a pulse generator

Systron Donner Model 100A Pulse Generator is test equipment. This instrument can generate pulse trains of various pulse widths and pulse repetition rates. It can also be triggered externally and produce a pulse with a variable delay after the occurrence of the trigger [34]. The instrument has the following features:

- Repetition rate from 0.1 Hz to 10 MHz
- Main output: Up to + 10 V amplitude, 5 ns rise time
- Variable width and delay to 10 sec
- Synchronous and asynchronous gating
- Normal and complementary outputs
- ± 250 mV trigger sensitivity

The pulse generator provided a negative rectangular pulse to test the operability of the preamplifier prior to the collection of data by the MCA.

3.1.4. CS – 2100 100Mhz 4-channel oscilloscope [35]

An **oscilloscope**, previously called an oscillograph, and informally known as a **scope**, **CRO** (for cathode-ray oscilloscope), or **DSO** (for the more modern digital

storage oscilloscope), is a type of electronic test instrument that allows observation of constantly varying signal voltages, usually as a two-dimensional graph of one or more electrical potential differences using the vertical or *y*-axis, plotted as a function of time (horizontal or *x*-axis). Many signals can be converted to voltages and displayed this way. Signals are often periodic and repeat constantly, so that multiple samples of a signal which is actually varying with time are displayed as a steady picture. Many oscilloscopes (storage oscilloscopes) can also capture non-repeating waveforms for a specified time, and show a steady display of the captured segment. CS- 2100 100 MHZ 4-Channel Oscilloscope is a product of Trio-Kenwood Corporation. The Cathode Ray Tube (CRT) has a display area of 8 x 10 div (1 div = 1 cm) and accelerating potential of 16 kV. The shape is rectangular, with internal graticule.

Oscilloscopes are commonly used to observe the exact wave shape of an electrical signal. Oscilloscopes are usually calibrated so that voltage and time can be read as well as possible by the eye. This allows the measurement of peak-to-peak voltage of a waveform, the frequency of periodic signals, the time between pulses, the time taken for a signal to rise to full amplitude (rise time), and relative timing of several related signals.

In this work, the oscilloscope was used to observe the output signals from the preamplifier and the main amplifier against signal overshoot and undershoot. The multi-channel analyzer (MCA) takes the very small voltage signal produced by the detector, reshapes it into a Gaussian or trapezoidal shape, and converts that signal into a digital signal.

3.1.5. Keithley model 263 calibrator / source [36]

The Keithley 263 Calibrator / Source is used as a secondary standard when calibrating electrometers and picoammeters. It also used for sourcing resistance, voltage, current and charge. Specifications of the Keithley 263 include:

- Source Current: 2 pA to 20 mA
- Resistance: 1 k ohm to 100 G ohm in 9 decade steps
- Voltage: 200 mV to 20 V
- Coulombs V/R (passive): 20 pC to 20 µC

The Keithley instrument was used to source inverting current values between 1 nA to 20 µA into the inputs of the current micro amplifiers of the two control systems to assess their stability and linearity.

3.1.6. Acculab ATL-124 Analytical Scale [37]

Acculab ATL-124 is an Electronic Analytical and Precision Balance with a weighing capacity of 120 g. The digital weighing scale has a readability of 1 mg and a tare range (subtractive) of 120 g. It has internal automatic calibration features as well as external calibration components. The Acculab ATL-124 analytical scale was used to weigh samples for irradiation.

3.1.7. Pneumatic Rabbit System for Sample Delivery [38]

There are 10 irradiation channels in the reactor, five inner irradiation channels which can take the sample capsule with volume 7 cm^3 and are uniformly distributed along a concentric circle with diameter of 330 mm in the side beryllium reflector. Five outer irradiation tubes are also installed outside the beryllium annulus.

Three of them can take capsule with volume 7 cm^3; the other two can take capsule with volume of 25 cm^3.

The system was used to transfer the flux monitors (^{197}Au) into the inner irradiation site two of the reactor core.

3.2. Methods

3.2.1. Calibration of multi-channel analyzer (MCA) of high purity germanium (HPGe) detectors

Detector calibration allows the gamma-ray spectrum to be interpreted in terms of energy. Calibration of MCA is necessary for the determination of the energy scale of pulse distribution. The easiest calibration method is to place sources of known energy on the detector and record the channel number into which the centroid of the resulting full-energy peak falls. The following known sources were used to calibrate the system: Barium -133, Cesium-137 and Cobalt-60. The sources were placed at the detector geometry of 5.0 cm and counted for 600 sec at a biasing voltage of – 4500 V. Three points calibration method was used. Other energy peaks were used to provide additional points along the line for confirmation purposes and testing of linearity.

3.2.2. Checking operationality of the preamplifier against signal undershoots

A charge – sensitive preamplifier of a gamma spectrometry system has a capacitor which charges the incoming pulse to the required voltage and discharge through a resistor depending on the decay time constant, τ which is controlled by the feedback network R_f C_f [35].

To test the operability of the preamplifier against signal undershoot, a negative pulse was fed through the test input of the preamplifier. The pulse should have a rectangular shape with amplitude of 100 mV and 1 ms pulse width. Perfect output signal was observed without undershoot.

Figure 3.1 shows the set up for the operating conditions for the test signal are:

Shape:	Rectangular
Polarity:	Negative
Amplitude:	100 mV
Pulse Width:	1 ms

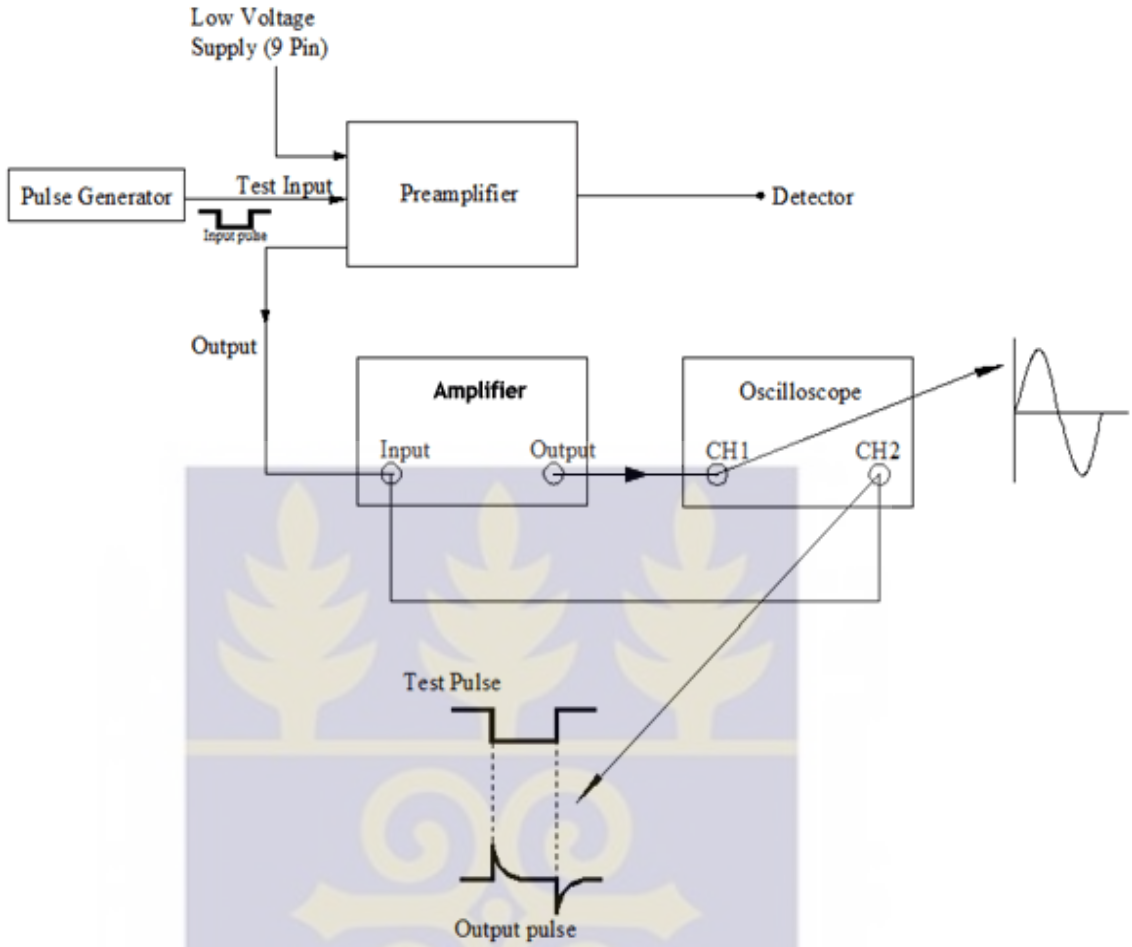

Figure. 3.1 Set-up for testing the preamplifier output signal against over and Undershoot

3.2.3. Calibration of micro-current amplifier using keithley model 263, calibrator / source

Ionized current produced in the small fission chamber is sent into a micro-current amplifier as shown in Fig. 2.3. After amplification, the current is converted into two output Voltages, V1 and V2. V1 represents the significant digits of the neutron flux, while the V2 represents the power of the neutron flux.

The fission chamber was disconnected from the control instrumentation including the high voltage. The Keithley model 263 calibrator / source instrument was used to

inject the following inverting current (I) values; 1000 pA, 25 nA, 3 µA, 10 µA, 15µA and 20 µA respectively into the input of the IC (ICL 7650) pin 4, the inverting input of the amplifier, representing the current pulses from the fission chamber to check the stability and linearity of the auto micro current amplifier. Readings were taken at each injection of the current and were tabulated (Tables 4.1).

The neutron flux displayed on the screen can be estimated from the relation

$$\text{Neutron flux displayed on the screen } (\Phi) = \frac{I(\mu A)xK}{10^{-12}A}(n/cm^{-2}s) \quad - \quad (3.1)$$

Where K = the sensitivity coefficient of the ionization chamber= 6.0 x 10^4 (for the MCCLS)

K = 5.0 x 10^4 for the control console (CC)

I (µA) = the pulse current from the ionization chamber measured in micro-amperes

Φ = neutron flux displayed on the screen of the CC and MCCLS

The factor 10^{-12} A is a change in ionization current

3.2.4. Neutron flux measurements

Thermal neutron fluxes were measured using a micro-fission chamber coated with enriched U^{235} placed in the inner irradiation site of the reactor. The fission chamber provide input signal in the form of current generated due to interaction of the thermal neutrons with the U^{235} coating which is calibrated against thermal neutron fluxes measured on the control systems.

Gold is composed of only one isotope, 197Au. When this isotope captures a neutron, it becomes radioactive 198Au, emitting beta particles and gamma rays. The half-life for this decay is 2.6943 days. Thus, gold is a convenient material for standard foils, especially if the foils are exposed at one site and transported to another site for counting.

In this work Au solutions and Au-Al wire were used. Gold solution was pipette into cotton in order to avoid of self-shielding; flux perturbation and flux sink due to negligible thickness. The gold solution was prepared by NIST. Seven sample monitors of gold solutions (concentration-1000 ppm) of masses between 1.1 x 10^{-4} g to 1.2 x 10^{-4} g were irradiated for neutron flux settings of 1.67 x 10^{11}, 3.33 x 10^{11}, 5.0 x 10^{11}, 6.67 x 10^{11}, 8.33 x 10^{11}, 1.0 x 10^{12} and at shut down (n/cm^{2}s), corresponding to 5 kW, 10 kW, 15 kW, 20 kW, 25 kW 30 kW and shut down power respectively in the inner irradiation site two of GHARR-1. Two replicates were prepared for each set of irradiation for both cadmium-covered and bare irradiations. Cadmium plate was first cut into rectangular shape according to the required measurement (2/1 height by radius) and folded into cylinder with both top and bottom cover. The polyethylene capsule was then placed in the cadmium cylinder such that all the surface area of the capsule was completely covered with 1mm thickness of cadmium. Au-Al wire of masses between 3.0 x 10-6g to 3.5 x 10-6g was also used to compliment Au monitor at 15 kW where the reactor is normally operated.

Flux at shut down was determined due to the fact that photo neutrons from the interactions of gamma rays through the (γ, n) reaction that provides a useful start-up source once the core is activated. There is always a residual power after shut-down

which would be investigated to assess the actual power through the neutron fluxes measured by the two control systems.

The reaction rate (R) per atom, for an isotope exposed to a mixed thermal and epithermal neutron field is given by:

$$R = R_s + R_{e,cd} = G_{th}.\sigma_0.\varphi_{th} + G_e.I_0(\alpha).\varphi_e \quad (3.2)$$

When a flux monitor is irradiated under 1mm cadmium foil, the activation rate is given as;

$$R_{e,cd} = G_e.I_0(\alpha).\varphi_e \quad (3.3)$$

Cadmium-covered activation fluent rate was used to eliminate the unknown epithermal component of the flux spectrum.

In this case, sub-cadmium reaction rate could be obtained by re-arranging equation (3.2) and (3.3) as;

$$R_s = R - R_{e,cd} = R - \frac{R_{e,cd}}{F_{cd}} = G_{th}.\sigma_0.\varphi_{th} \quad (3.4)$$

The thermal fluence rate of gold solution (pipette onto cotton) which had been irradiated with and without cadmium cover was then calculated as follows;

$$\varphi_{th} = \frac{1}{G_{th}\sigma_0}\left(R - \frac{R_{e,cd}}{F_{cd}}\right) \quad (3.5)$$

Where,

$$R \text{ or } R_{e,\,cd} = \frac{C \exp(\lambda t_w)}{(\varepsilon N_0 (1 - \exp(-\lambda t_i)))} \qquad (3.6)$$

the reaction rate per target atom (for both bare and cadmium-covered irradiation respectively).

3.2.5. Irradiation, counting and interpretation of flux monitors

Each Monitor, the (cadmium covered and bare respectively) was irradiated for 1hr and 30 minutes and allowed to decay within a day before data acquisition was made on the HPGe detector for 3600 and 1800 seconds set live time respectively. This will enable the ADC of the MCA to process the gamma pulses using a shorter dead time and cut off the larger pulses above the upper discrimination set line. Determinations of the flux parameters were done by using cadmium ratio dual-monitor method.

The cadmium ratio method was used to determine the thermal and epithermal neutron flux density. Specific net area under the full peak energy 411.8 keV and 724+756 keV from reaction $^{197}Au\ (n, \gamma)\ ^{198}Au$ was interpreted with WinSPAN.

Dimensions of the cadmium cylinder used

- Length = 4.7 cm
- Thickness = 1 mm
- Height = 2.65 cm
- Inner diameter = 1.45 cm
- Radius = 0.725 cm
- Volume = 4.38 cm^3

Capsules used

- Large cylindrical polyethylene capsule, height = 5.55 cm
- Inner diameter = 1.5 cm
- Outer " = 1.65 cm
- Small cylindrical polyethylene capsule, height = 2.35 cm

  (Half that capsule was used)
- Inner diameter = 1.05 cm
- Outer " = 1.2 cm

Measurements were done using calipers.

3.2.6. Temperature and neutron flux measurement

GHARR-1 was operated at the following power levels: 5 kW, 10 kW, 15 kW, 20 kW, 25 kW and 30 kW using two control systems, the control console (CC) and the micro computer close loop systems (MCCLS) independently. Thermal-hydraulics and neutronics parameters were monitored and readings taken at 5, 10 and 20 minutes intervals on both control systems at steady state. Parameters monitored were; inlet temperature, outlet temperature and temperature change across the core. Other parameters were the; control rod position and neutron fluxes at various power levels.

Readings were also taken from the two neutronics meters of the control systems after 48 hours of reactor shut down.

Mastech digital multimeter (MAS-345), an auto ranging professional measuring instrument with temperature measuring option was used to measure the inlet

temperature alongside what was being measured by the meters in the control systems.

The reactor water was drained by the purification plant and its temperature measured using thermometer after 64 days of reactor shut down. The results were compared with the reading taken using the mastech-345 and the readings on the consoles.

3.3. Determination of core excess reactivity at critical power

Experimental data on rod position and its corresponding cold core excess reactivity were obtained at a critical control rod position of 137 mm and 2.55 mk respectively. The corresponding neutron flux at the critical rod position was 1.0×10^9 n/cm^2s. The excess reactivity was calculated from the start up excess reactivity verses critical control rod position to confirm earlier experiment figure 4.4.

3.4. Transient and steady state analysis on GHARR-1

The validity of the correlations between temperature and power as well as neutron flux and power, were investigated at steady and transient states shown in Eqs. 3.7 & 3.8 respectively. Dynamic experiments were performed to investigate the effects of insertions of step and ramp reactivities on Ghana Research Reactor-1.

The following correlation predicts the reactor fission power based on the neutronics parameter :

$$P = 3.1 \times 10^{-10} \Sigma_f V_f \Phi \quad - \quad (3.7)$$

Where Φ = average thermal neutron flux in the inner irradiation channel (n/cm^2s)

V_f = volume of the core = $\pi r^2 h$ (cm^3)

Core height (h) = 23 cm

Core radius (r) = 11.55 cm

$\Sigma_f = N_f$ (microscopic fission cross section of the core = 1.013 x $10^{-2}cm^{-1}$)

$$\Delta T = (5.725 + 147.6H^{-2.64})T_i^{-0.35}P^{(0.59+0.0019T_i)} \quad - \quad (3.8)$$

Where ΔT = Temperature difference between inlet and outlet orifices (^oC)

H = Height of the inlet orifice (mm)

T_i = Inlet temperature (^oC)

The correlation of power and temperature difference across the core ΔT (^oC)

Used for this work.

$$\Delta T = 6.81T^{-0.35}P^{(0.59+0.0019T_i)} \quad - \quad (3.9)$$

Thus, from equation (3.9)

$$P = Exp\left[In\left(\frac{\Delta T}{6.81T_i^{-0.35}} \right)(0.59 + 0.0019T_i)^{-1} \right] \quad (3.10)$$

In the experiments, two types of reactivities were released to examine the rising, drifting and damping of the reactor power in order to access its self-regulating capability. Step experiment was carried out by pumping two cadmium (Cd) rabbits with the reactivity worth of 2.1 mk into two inner irradiation sites of the reactor. The reactor was started and its central control rod was raised until the reactor was critical at a flux of 5.0 x 10^9 n/cm^2s and critical rod position of 151 mm. The prevailing

condition was maintained for some time and the two Cd rabbits were suddenly pumped out almost at the same time.

With the ramp experiment which involved the release of quasi-linear reactivity of 4 mk, the control rod was withdrawn from the bottom of 0.0 mm to the upper limit of 230 mm. GetData Graph Digitizer Version 2.24 software was used to reproduce the graphs for further analysis.

CHAPTER 4

RESULTS

In this chapter, the results obtained from the various experiments are presented in a logical sequence using tables and figures. The chapter emphasizes on important observations or summary of the tables and figures in the text. Only data generated from this study are presented.

4.1. Calibration results of spectrometry system for gamma energy measurements

The primary objectives of calibration are to ensure that an instrument is working properly and hence will be adequate for its intended purpose and also to adjust the calibration factor, if possible, so that the overall measuring precision of the instrument is optimized.

If a gamma spectrometer is used for identifying samples of unknown composition, its energy scale must be calibrated first. Calibration was performed by using the peaks of known sources (standard), such as barium-133, cesium-137 and cobalt-60. Because the channel number is proportional to energy, the channel scale can then be converted to an energy scale. Barium source was used to enable the MCA card to detect energies of low values. Lead absorbers were placed around the measuring apparatus to reduce background radiation. Figure.4.1 shows the linearity of the MCA. The graph takes a linear or proportional relationship in a form $y = mx + c$ which implies that the MCA with the gamma spectrometry system are in good condition and hence suitable for its intended purpose.

The equipment used in the gamma spectroscopy includes an energy-sensitive radiation detector, electronics to collect and process the signals produced by the detector, such as a pulse sorter (i.e., multichannel analyzer), and associated amplifiers and data readout devices to generate, display, and store the spectrum (as shown in figure.2.12)

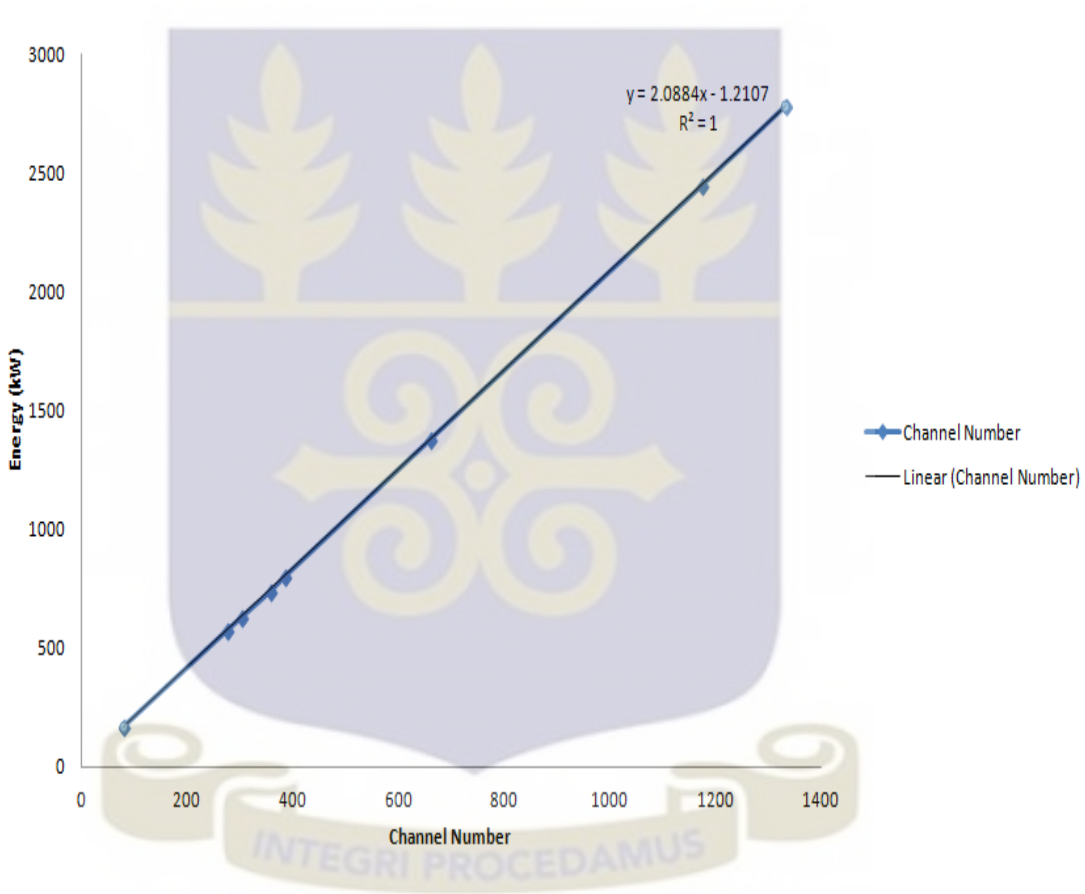

Figure.4.1 Calibration curve of energy against channel of MCA in spectrometry system for gamma energy measurements

4.2. The decay time constant of the exponential signal at the preamplifier output

The figure. 4.2 below shows that the rectangular test pulse of amplitude 100 mV and pulse width of 1 ms has given a perfect output of a RC differentiated signal for presentation to a main amplifier [35].

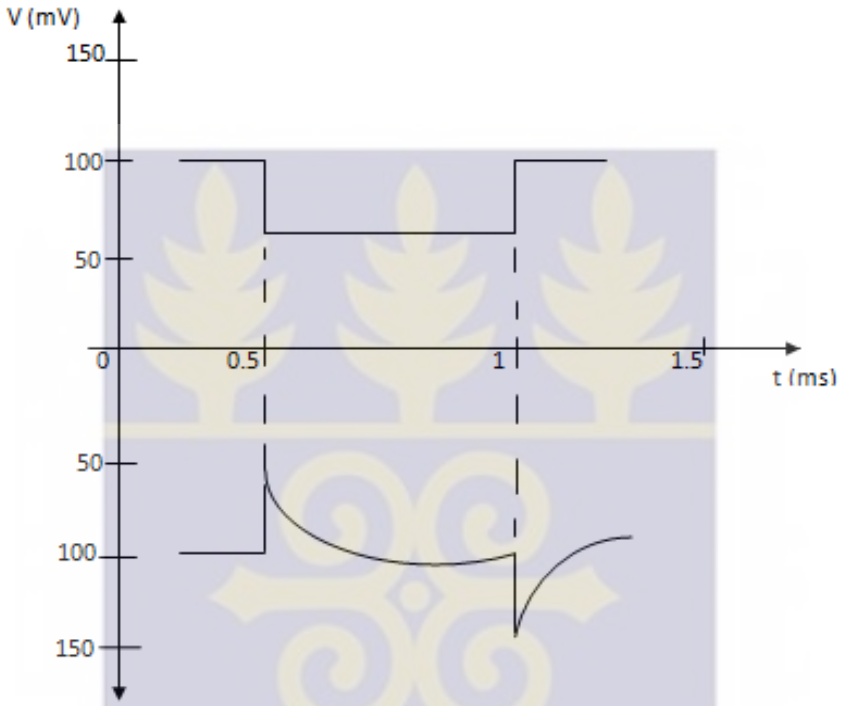

Figure. 4.2 Perfect output signal of charge – sensitivity preamplifier with test rectangular input pulse

4.3. Variations in neutron fluxes between the control console (CC) and micro computer close loop system (MCCLS)

It was observed from the sensitivity experiment conducted on the two (2) micro current amplifiers that the control systems, the control console and the micro-computer closed loop systems operate independently. The sensitivity coefficients of

the ionization chamber used for the MCCLS and CC were 6.0 x 10^4 and 5.0 x 10^4 respectively, at a neutron flux corresponding to a 10^{-12}A change in ionization current.

As a result, the two micro amplifiers give different voltage output readings corresponding to a particular neutron flux. A Keithley instrument was used to inject 10μA corresponding to 5.0 x 10^{11} n/cm^{2}s (15kW) by calculation into the micro amplifiers of the two independent control systems. The values registered on the meters of the CC and the MCCLS were 6.07 x 10^{11} and 5.03 x 10^{11} n/cm^{2}s respectively. The difference is as a result of the sensitivity coefficients and this has necessitated for the provision of a flux conversion factor of 1.2 which was used in dividing readings of the MCCLS to ensure same readings on the meters. Figure. 4.3 give a clearer picture of the difference between the two readings of the amplifiers. Table 1B in the appendix 1 also explains it.

From the operational log books (1999-2000) of previous control system, it was observed that at a preset fluxes of 5.0 x 10^{11} and 1.0 x 10^{12} n/cm^{2}s corresponding to 15 kW and 30 kW respectively, neutron flux meter of the MCCLS displays about 6.511 x 10^{11} and 1.257 x 10^{12} n/cm^{2}s respectively while the CC displays about 5.03 x 10^{11} and 1.0 x 10^{12} n/cm^{2}s respectively. The difference between the old control system (MCCLS) and the new one was that, the conversion factor of 1.2 has to be multiplied manually while as in the new one, the conversion factor has been incorporated in the software.

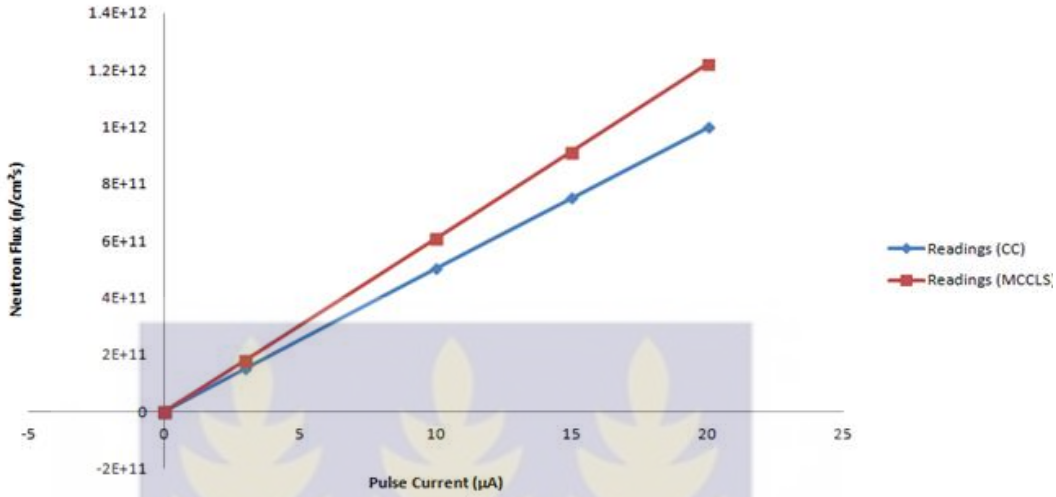

Figure. 4.3 Neutron flux with pulse current for CC and MCCLS

4.4. Experimental results of thermal neutron flux measurements

The determination of neutron fluxes in an irradiation channel is necessary to monitor the continuous stability of the nuclear reactor flux (required for neutron activation analysis).

The reactor was operated at critical power of 30 Watts (1.0×10^9 n/cm^{2}s) assessing the state of the reactor core regarding its core reactivity worth. Core excess reactivity of 2.55 mk was measured instead of the design rating of 4 mk. The reduction of 36.3 % in core excess reactivity was due to fuel depletion. Fig. 4.4 was used to determine the reactivity.

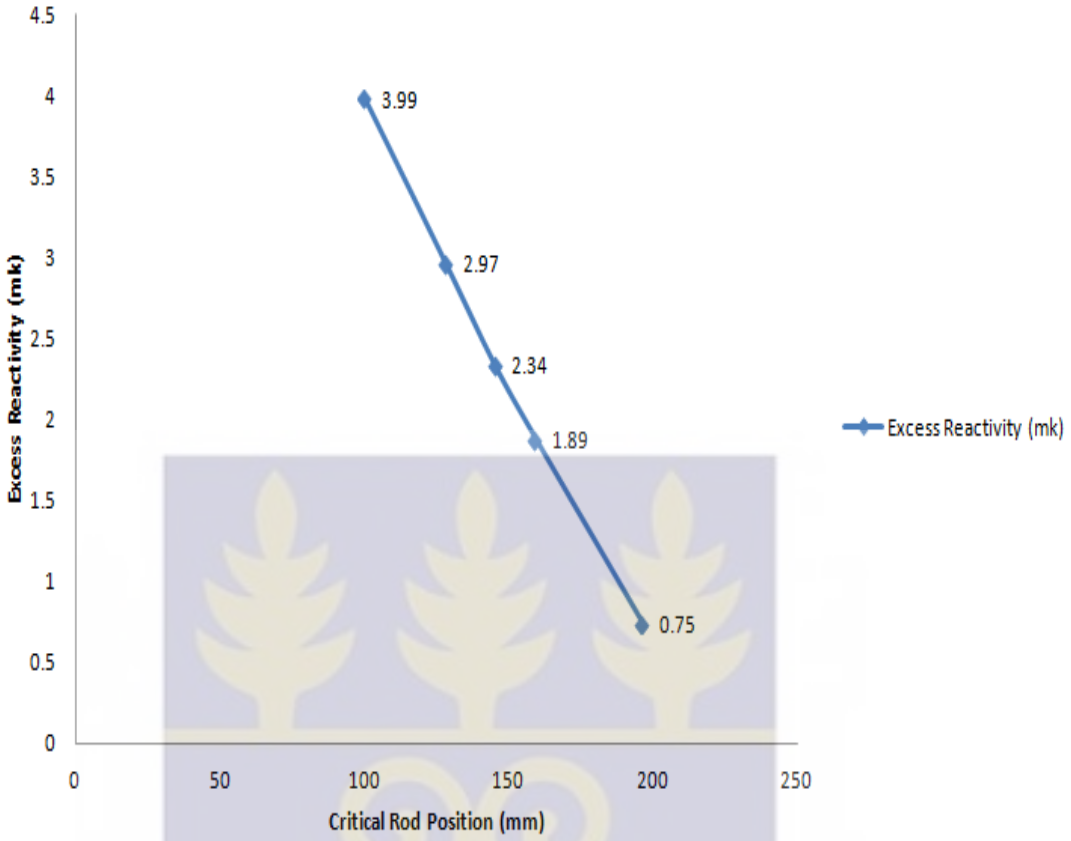

Figure. 4.4: Core Excess Reactivity with Critical Rod Position

In order to assess the actual neutron flux population in the reactor core and compare with what the meters displayed at a particular power level, a gold solution (^{197}Au) was sent into the inner irradiation site two (2) as flux monitor. The result as shown in figure. 4.5 indicate some variations in the flux values between what were in the core and that registered on the meters. The deviation has a mean error value of 36.5% against 36.3% decrease of core excess reactivity during the experiment. There was a good agreement between the flux monitor values and the reading of the core excess reactivity at critical power. The CC and MCCLS read almost the same neutron flux as preset on the control systems. The values on the meters were different

from the experimental flux monitor measured values which was about 1.6 times the flux registered on the neutron flux meters.

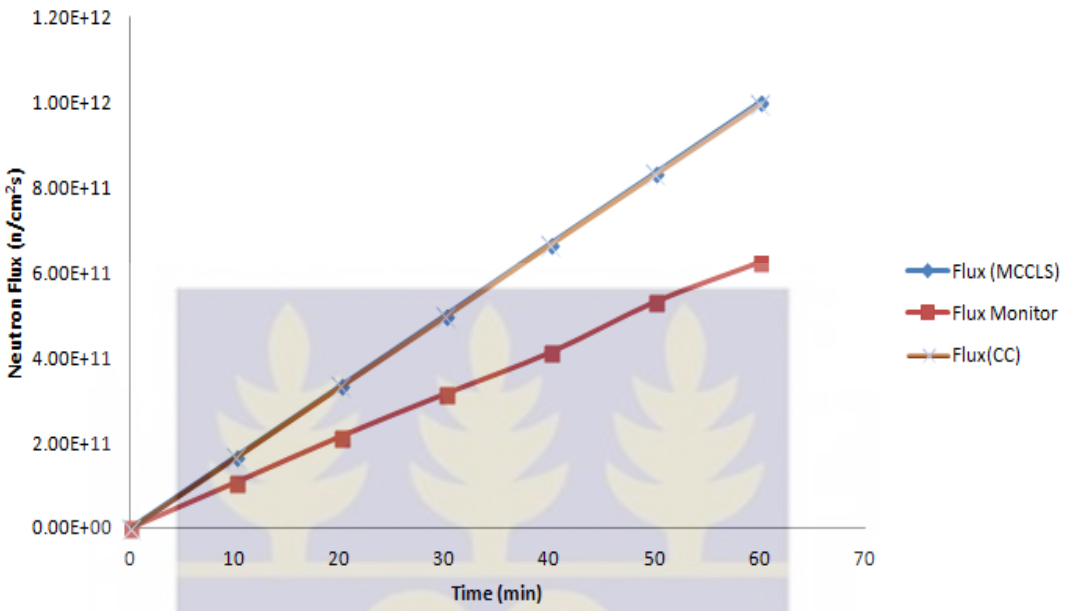

Figure. 4.5 Variation of neutron fluxes with time for CC and MCCLS.

Table 4.1 Variation in measured neutron flux and the experimental flux at the reactor inner site 2 at core excess reactivity of 2.55 mk

Thermal Power (kW)	Thermal Neutron flux (n/cm^2s)	Experimental values using flux monitor (n/cm^2s)	Percentage decrease in neutron flux (%)
5	1.67E+11	1.07E+11	35.93
10	3.33E+11	2.15E+11	35.44
15	5.00E+11	3.15E+11	37.00
20	6.67E+11	4.21E+11	36.89
25	8.33E+11	5.31E+11	36.25
30	9.99E+11	6.24E+11	37.54
			MEAN = 36.5

4.5. Reactivity adjustment

The reactivity of 2.55 mk obtained from operating the reactor at critical prompted the operating institute to adjust the four (4) reactivity regulators in order to increase the core reactivity to 3.99 mk. Au-Al wire was used as another monitor at irradiation site 2 of the reactor core at 15 kW where the reactor is normally operated. The monitor was used before and after operation at 15 kW. The results obtained before and after the adjustment were 3.20 x 10^{11} n/cm^{2}s and 4.68 x10^{11} n/cm^{2}s respectively.

4.6. Control system response to measurements at different power levels at steady State

Figure.4.6 below shows a corresponding increase of reactor neutron fluxes against reactor thermal power from 5 to 30 kW. The preset neutron fluxes measured by the CC and MCCLS were the same but at different control rod positions, tables 4.4 and 4.5.

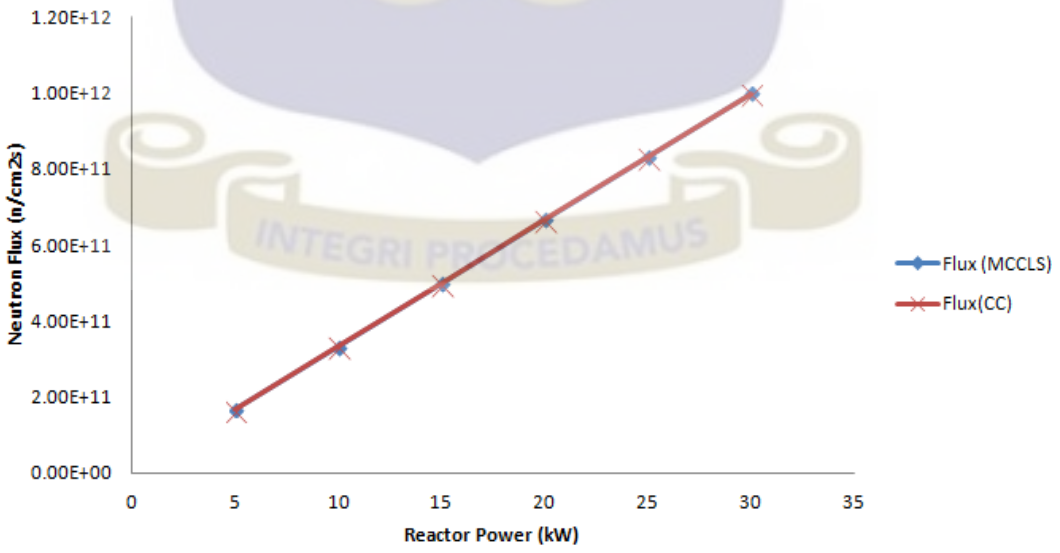

Figure. 4.6 Neutron fluxes variation against thermal power at different levels for CC and MCCLS

4.7. Control system behaviour with respect to flux levels and coolant temperature at steady state

After shutting down the reactor for about 64 hrs, it is expected that the reactor coolant temperature becomes uniform in the reactor vessel. It was observed that the meters in the two control systems measured different readings when the reactor instrumentations were switched on. From figure 4.7 it was observed that at flux 5 x 10^{11} n/cm^{2}s MCCLS meter read 36 ^{o}C whereas CC meter read 32 ^{o}C, difference of 4 ^{o}C. Temperature change will occur in the two meters only when the reactor is operated after 30 min due to the locations of the various temperature probes (as shown in figure. 2.14). The inlet temperature probe of MCCLS is fixed at inlet orifice of the core whereas the CC temperature probe is fixed some distance above the core.

The erratic behavior of the inner temperature of MCCLS led to the replacement of an integrated circuit (IC) U10D [36] and re-soldering of the sensor TMP_{36}. The IC is a Wide-Bandwidth JFET-Input Quad Operational Amplifier (LM 837). The cold leg of the inlet thermocouple was at room temperature and was compensated. TMP_{36} temperature sensor is used to measure the room temperature and transmitted to ADC12 (figure. 2.11) through U10D (LM 837) which amplified the signal. The readings of the two meters of inlet temperatures observed to be in perfect agreement (Figures. 4.7 and 4.8).

Figures. 4.9 and 4.10 show the system behavior with respect to flux levels and coolant temperature. The coolant temperature increased gradually with increase in

neutron flux due to fission process and rise sharply due to the water circulation from the inner orifice of the core to the outer orifice.

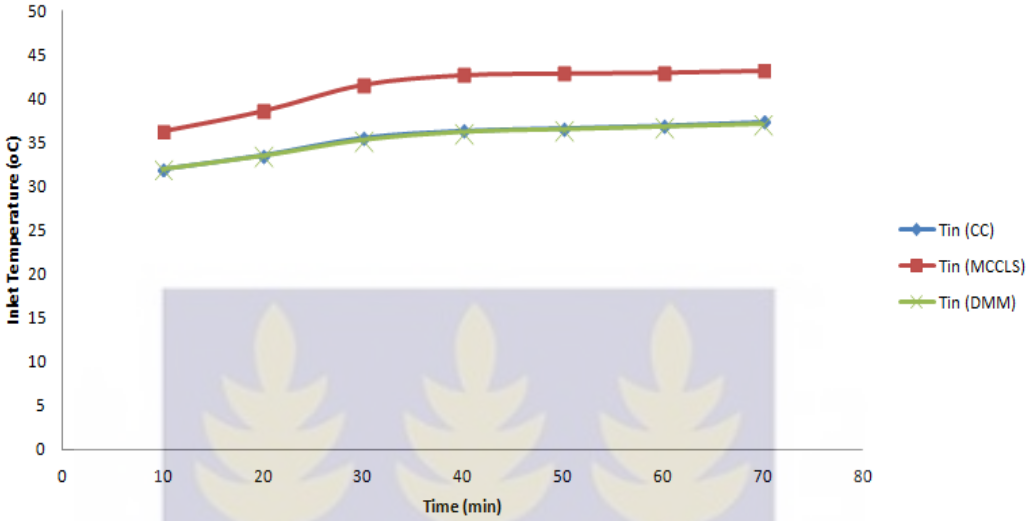

Figure.4.7 Variation of average inlet temperatures with time for (CC), (MCCLS) and digital multi-meter (DMM)

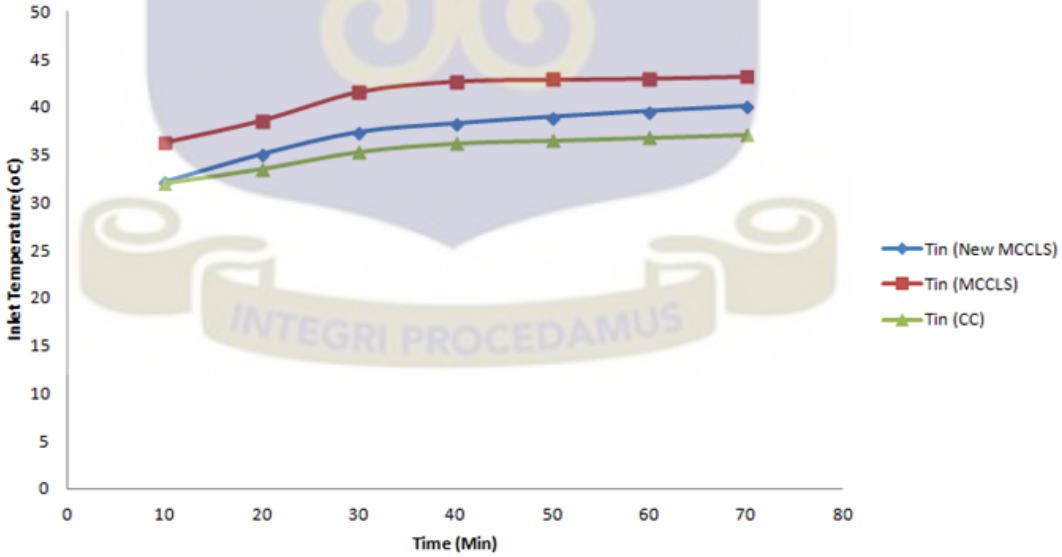

Figure. 4.8 Variation inlet temperatures with time for CC and MCCLS after the replacement of new IC for neutron flux of 5.0 x 10^{11} n/cm^{2}s at steady state

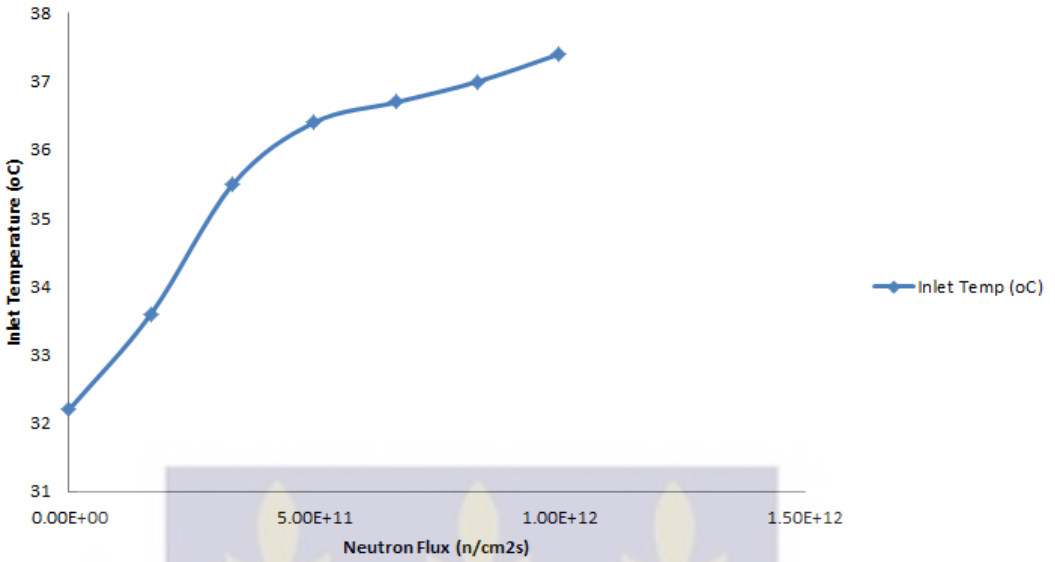

Figure. 4.9 Behaviour of neutron flux levels against the inlet coolant temperature on the CC

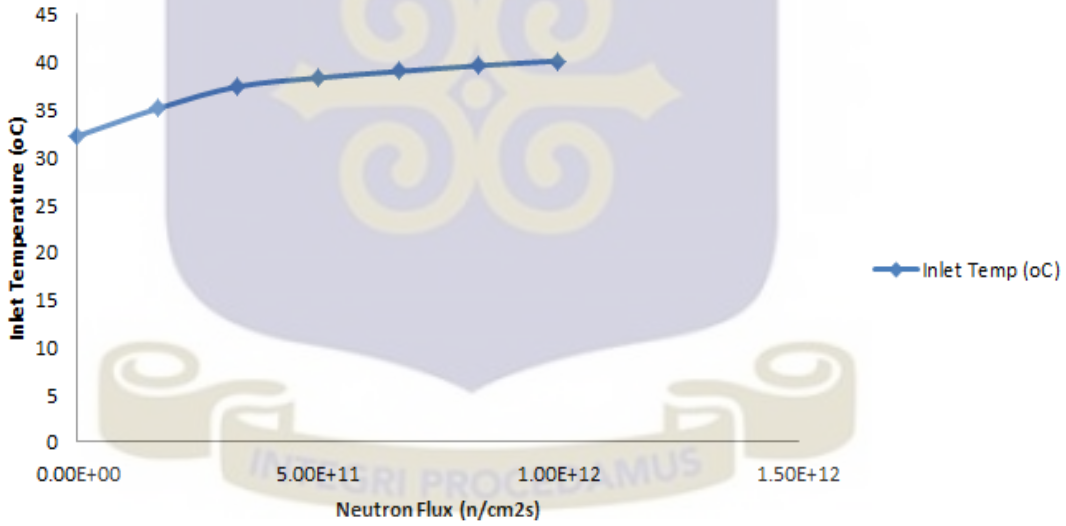

Figure. 4.10 Behaviour of neutron flux levels against the inlet coolant temperature on the MCCLS

Figures. 4.11 and 4.12, the outlet temperature against the neutron flux having the same flow pattern.

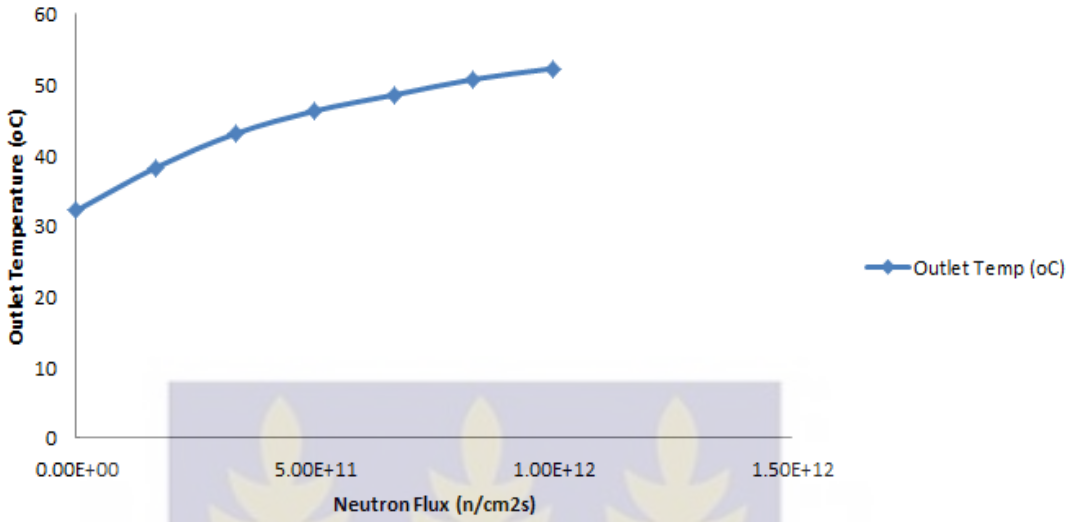

Figure.4.11 Behaviour of neutron flux levels against the outlet temperature on the CC

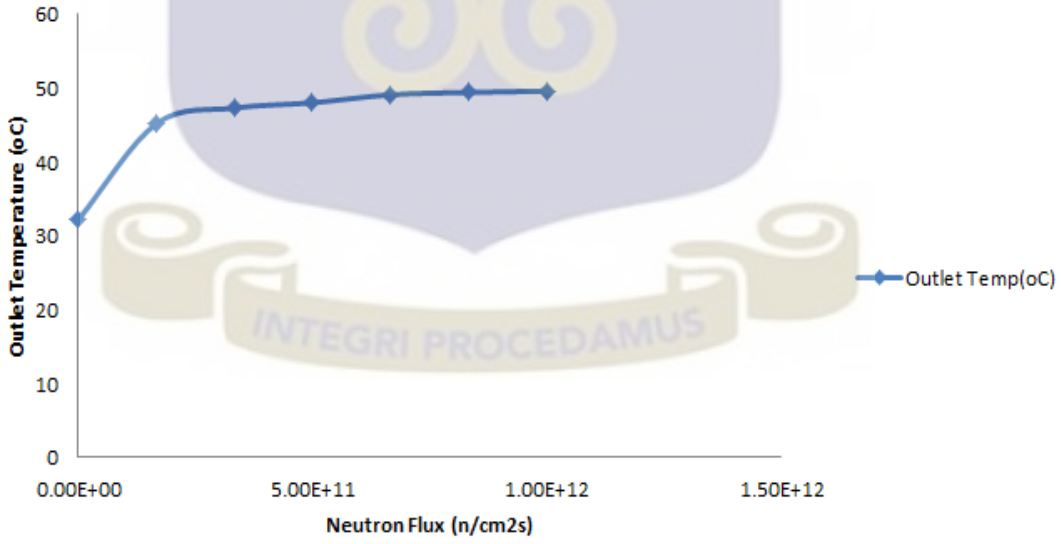

Figure.4.12 Behavior of neutron flux levels against the outlet temperature on the MCCLS

It can be seen from figures. 4.13 and 4.14 that, the temperature difference ΔT (^{o}C) across the reactor core is directly proportional to the thermal power of the reactor. Any change in the temperature affects the power value. Extrapolating the graph, the reactor thermal power and the neutron flux parameters could be predicted at any ΔT (^{o}C) value.

4.8. Variations of temperature difference with power across the core

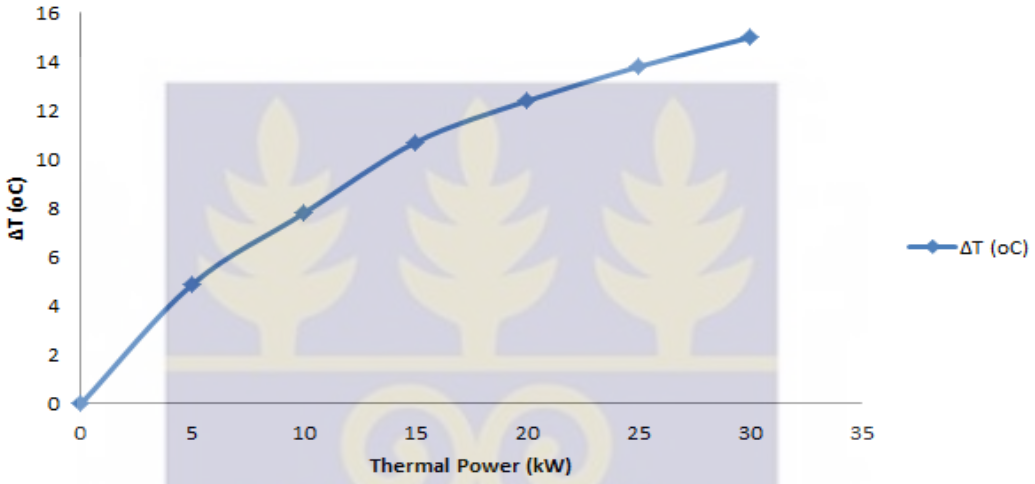

Figure. 4.13 Increase in temperature difference across the reactor core ΔT (^{o}C) against the increase in thermal power (kW) for CC at steady state

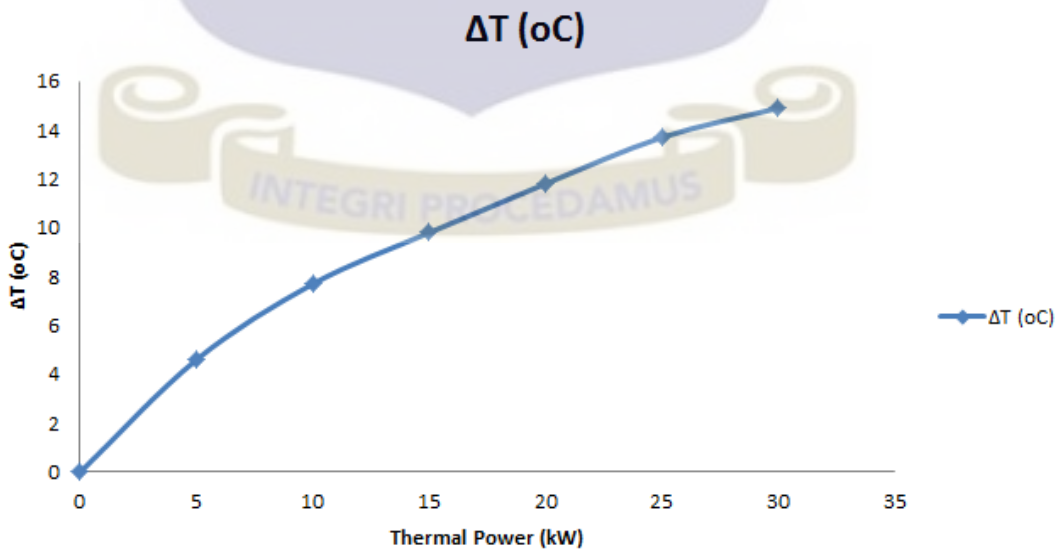

Figure. 4.14 Increase in temperature difference across the reactor core ΔT (^{o}C)

against the increase in thermal power (kW) for MCCLS at steady state

4.9. Variations of inlet temperature and temperature difference across the reactor core with time

Figures 4.15 – 4.17 explains the variations in the inlet temperatures with time against the temperature difference across the core since inception of the operation of the reactor. Inlet temperature readings since 1999 follow almost the same pattern. The temperature across the core varies or decreased after the replacement and upgrade of the old micro-computer close loop system (MCCLS) and other components in 2008, table 4.3. This affected the thermal power prediction using the correlation (3.9).

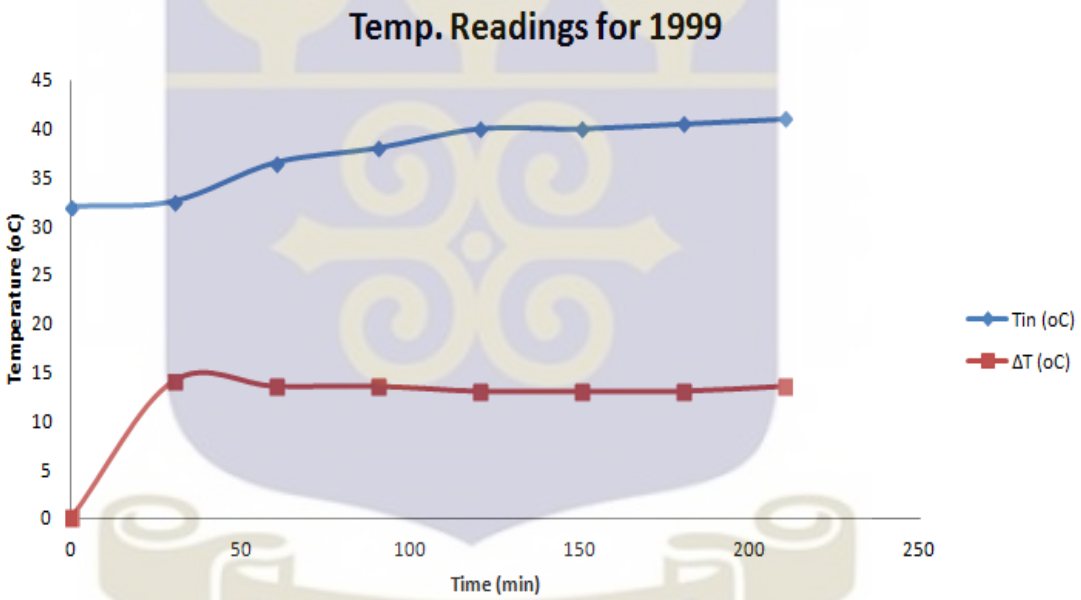

Figure.4.15: Temperature variations with time for 15 kW

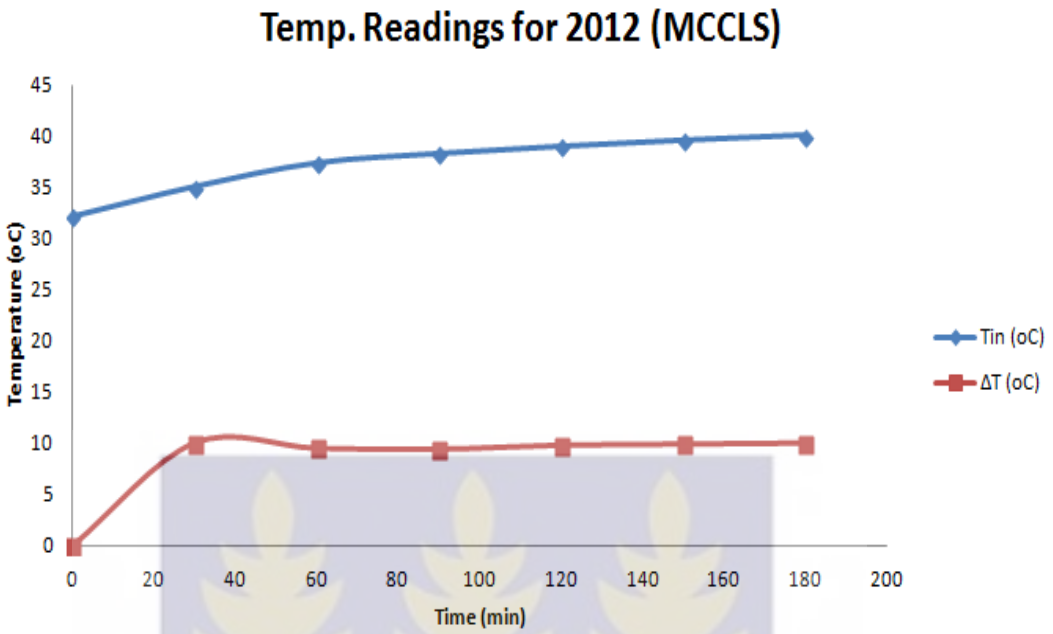

Fig.4.16: Temperature variations with time for 15 kW (MCCLS)

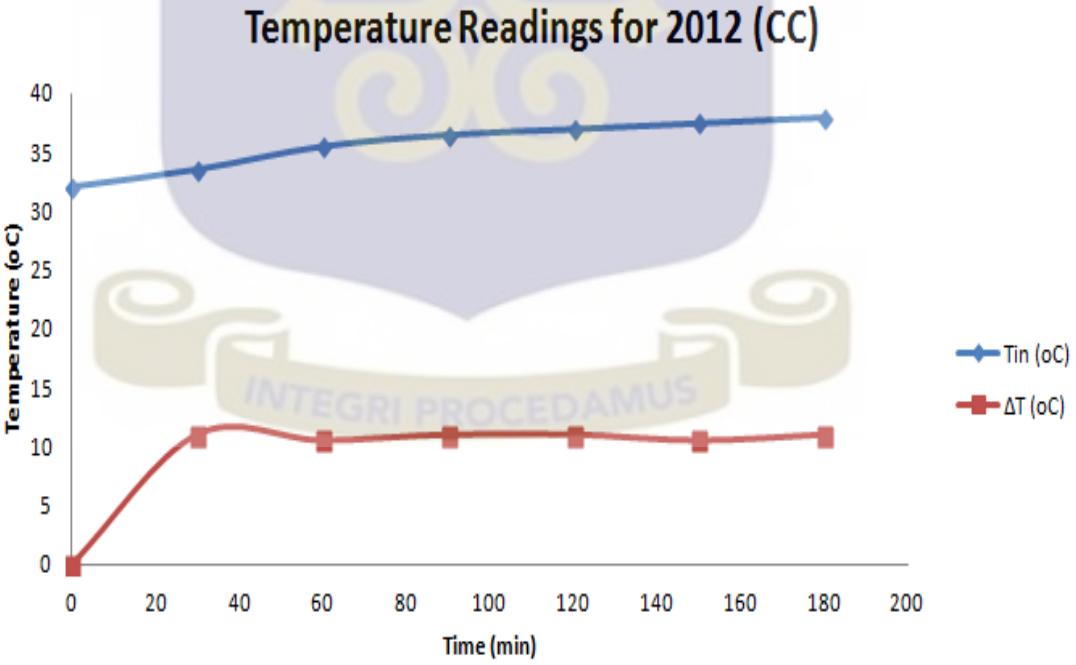

Fig. 4.17: Temperature variations with time for 15 kW (CC)

4.10. Variations of reactor rated power with the neutronic and the thermal power using the temp. correlation.

In light water research reactors, the water around the core serves as moderator and coolant. If the temperature of the coolant increases, the water molecules become less dense and the neutron flux begin to leak out. In order to keep the neutron flux (power) constant, the control rod moves up to release more neutrons to compensate for the loss due to fuel burn-up and samarium poison (Table 4.2). It could be deduced from the explanation that changes in temperature across the core as a result of nuclear fission is directly proportional to the thermal power. As the temperature increases, there is a corresponding increase in the leakages of neutron fluxes.

Upgrading the MCCLS by 2008, results show that the temperature difference decreased with thermal power. Ageing of the system might have contributed to increase in temperature difference and the thermal power from 1999 to 2008. Change in the height of the inlet or outlet orifice of the core due to either ageing of the beryllium or structural design problem. It can also be attributed to the removal of the aluminium tray on top of the core during beryllium addition.

Table 4.2: Neutronics and thermal-hydraulic parameters before and after the upgrade of the micro computer closed loop system (MCCLS)

Year	Flux Preset (n/cm^2s)	MCCLS (n/cm^2s)	CC (n/cm^2s)	Rod Position (mm)	Inlet Temp (°C)	ΔT (°C)	Thermal Power (kW) using Eq.[3.9]
1999	$5.0x10^{11}$	$6.42 x10^{11}$	$5.01 x 10^{11}$	129	31.0	13.5	18.2
2000	"	-	$5.00 x10^{11}$	138	33.0	13.0	17.5
2001	"	-	"	143	33.0	12.5	16.5
2002	"	-	"	149	32.0	13.2	17.8
2003	"	-	$5.01 x 10^{11}$	144	30.2	13.0	17.1
2004	"	-	"	149	29.5	12.5	16.0
2005	"	-	$4.99 x 10^{11}$	174	32.0	12.5	16.3
2006	"	-	$5.02 x 10^{11}$	160	30.0	13.0	17.1
2007	"	-	"	163	31.0	13.0	17.2
2008	"	-	$5.01 x 10^{11}$	172	29.5	12.5	16.0
2009	"	$5.00 x 10^{11}$	-	176	31.9	10.4	12.3
2010	"	"	-	156	32.3	10.5	12.5
2011	"	$4.99 x 10^{11}$	-	138	33.0	10.1	11.9
2012	"	"	-	143	31.0	10.0	11.5
2013	"	$5.00 x 10^{11}$	-	165	31.2	10.6	12.6

4.11. Variations of experimental neutron flux measured at shut-down with readings by two meters of the control systems

From table.4.3, two reading meters of the control systems, control console (CC) and micro computer closed loop system (MCCLS) measured 2.50 x 10^7 and 1.73 $x10^8$ n/cm^2s respectively at shutdown after two and half days. The experimental flux monitor (^{197}Au solution) sent into the inner irradiation site 2 of the core for 23 hrs

measured a flux of 1.18 x 10^{6} n/cm^{2}s corresponding to neutronics power of 35 x 10^{-3} Watts. This is the residual neutron flux in the core at the time of shut down which starts up the reactor without the application of a neutron source. The residual flux is the photo neutrons from the interactions of gamma rays through the (γ,n) reaction that provides a useful start-up source once the core is activated.

The difference in the flux magnitude of the two control systems is due to their measuring precisions. The MCCLS has a neutron flux measuring precision within a range of 5.0 x 10^{-9} A to 5.0 x 10^{-4} A, corresponding to 10^{8} to 10^{13} n/cm^{2}s. The control console also has relatively high measuring precision ranging from 5.0 x 10^{-10} A to 5.0 x 10^{-4} A, corresponding range of 10^{7} to 10^{13} n/cm^{2}s.

Thermal-Hydraulics and Neutronics Parameters Measurements

GHARR-1 was operated between power levels: 5 - 30 kW using two control systems, the control console (CC) and the microcomputer close loop systems (MCCLS) independently. Thermal- hydraulics and neutronics parameters were monitored and readings taken at 5, 10 and 20 minutes intervals on both control systems at steady state. Parameters taken were; inlet temperature, outlet temperature, temperature change across the core and neutron fluxes at various power levels, tables 4.3. The semi-empirical relationship between the reactor power, flux parameters, core inlet temperature and the coolant temperature rise Eqs. (3.7) and (3.9) was used to determined or predicted the actual neutronics and thermal powers shown in table 4.3. The readings on the meters of the control systems were used for the prediction.

Table 4.3 Data obtained from neutronics and thermal-hydraulics experiment conducted using CC and MCCLS from shutdown to 30 kW at steady state

Rated Power (kW)	Mean Measured Neutron Flux (CC) n/cm^{2}s	Mean Measured Neutron Flux (MCCLS) n/cm^{2}s	Flux Monitor at Different Rated Power levels n/cm^{2}s	Experimental Neutron Power (kW)		Experimental Thermal Power Using Temp. Correlation (kW)		Mean Inlet Temp. For CC (^{o}C)	Mean Inlet Temp. For MCCLS (^{o}C)	Mean Change in Temp. For CC ΔT (^{o}C)	Mean Change in Readings For MCCLS ΔT(^{o}C)	Mean Digital Multimeter Of Inlet Temp. (^{o}C)
				CC	MCCLS	CC	MCCLS)					
5	1.67x10^{11}	1.67x 10^{11}	1.07x10^{11}	5.01	5.01	3.96	3.85	33.6	38.5	4.9	4.6	33.5
10	3.33x10^{11}	3.33x 10^{11}	2.15x10^{11}	10.02	9.99	8.23	8.45	35.6	41.6	7.8	7.7	35.3
15	5.00x10^{11}	5.00x 10^{11}	3.15x10^{11}	15.00	15.03	13.57	12.11	36.4	42.7	10.8	9.8	36.2
20	6.68x10^{11}	6.67x 10^{11}	4.21x10^{11}	20.04	20.01	16.78	16.07	36.7	42.9	12.4	11.8	36.5
25	8.33x10^{11}	8.33x 10^{11}	5.31x10^{11}	24.99	24.99	19.82	19.95	37.0	43.0	13.8	13.7	36.8
30	9.98x10^{11}	9.99x 10^{11}	6.24x10^{11}	29.94	29.97	22.46	22.75	37.4	43.2	15.0	14.9	37.1

4.12. Correlations between flux and power, temperature and power at transient state.

The step experiment of 2.1 mk reactivity insertion in the reactor core gave rise to a temperature difference across the core from 0.2 to 21.6 ^{o}C and neutron flux from 3.98 x 10^{9} to 1.23 x 10^{12} n/cm^{2}s. Figure. 4.18 and 4.19 show clearly the variations in the power due to neutron flux and power due to thermal hydraulics from start to about 23% above the rating (30kW). The two correlations, Eqs. (3.7) and (3.9) gave almost the same thermal powers but vary at a higher temperature difference across the core.

Ramp experiment of 4.0 mk reactivity insertion in table 3C gave a different picture regarding power variations. The disparities are clearly seen in figures 4.20 and 4.2.

The correlation between neutron flux and power, as well as temperature and power produce almost the same thermal power at about 23% above the rating power but deviate at lower and higher power ratings. It was observed that the difference in temperature across the core ΔT is directly proportional to the thermal power P.

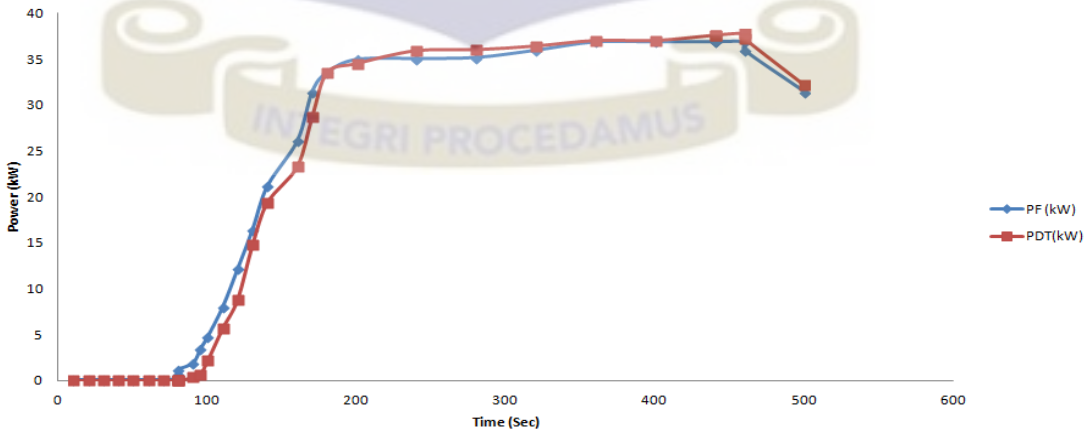

Figure.4.18 Variation of GHARR-1 power, with the neutron flux (P_F) and temperature (P_{DT}) reactivity released of 2.1 mk at transient state

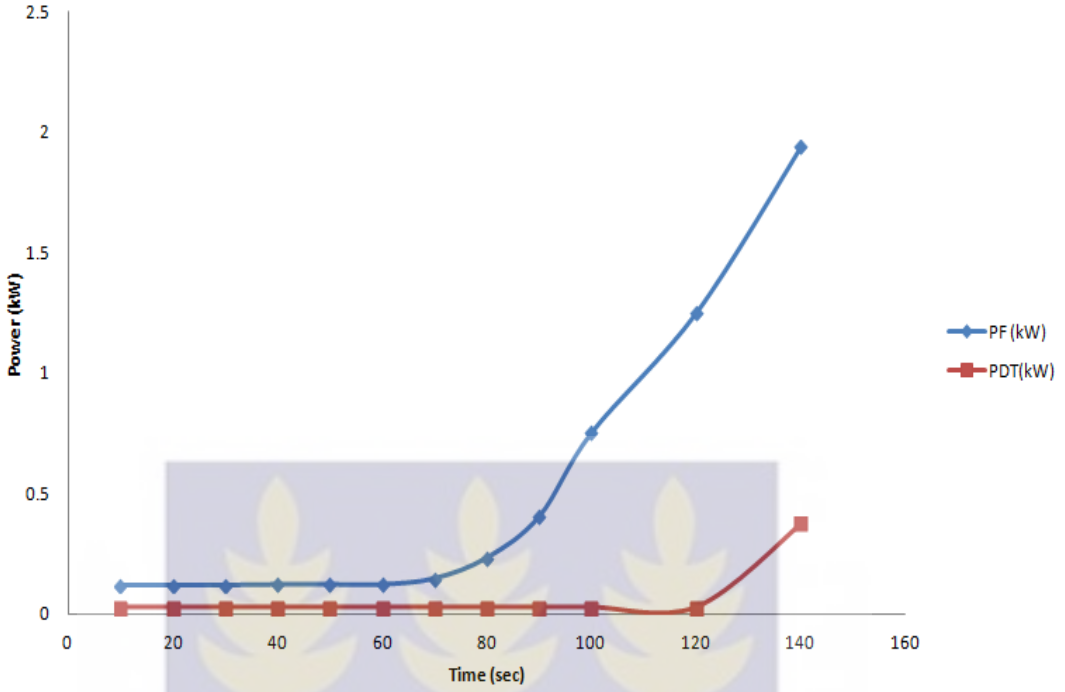

Fig. 4.19 Variation of GHARR-1 power, with the neutron flux (PF) and temperature correlation (PDT) for reactivity released of 2.1 mk at very low power at transient state

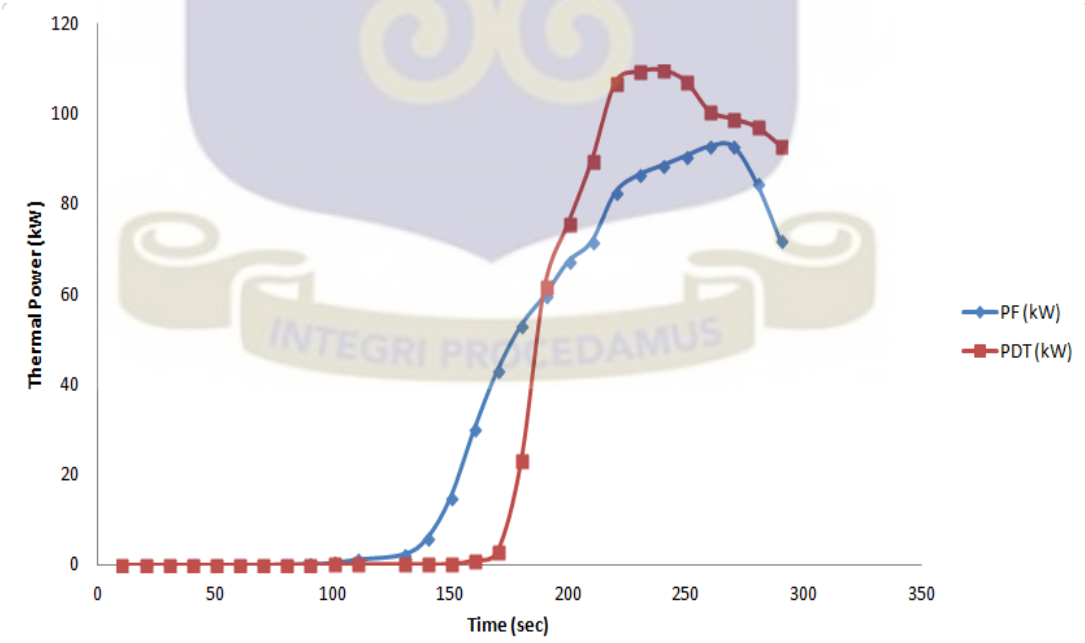

Fig. 4.20 Variation of GHARR-1 power with the flux (P_F) and temperature (P_{DT}) correlation at a reactivity release of 4.0 mk at transient state

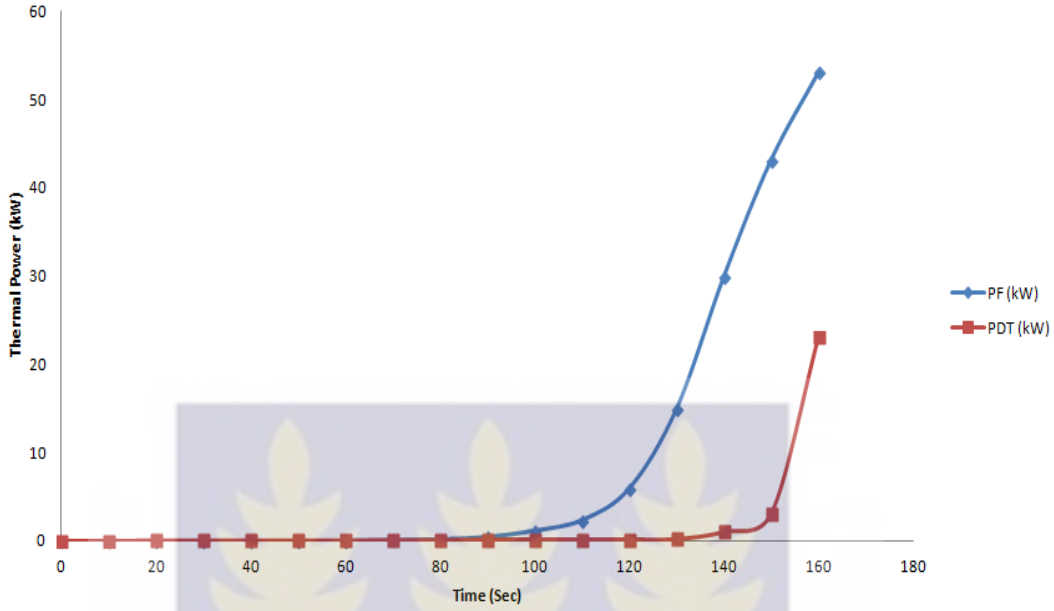

Fig 4.21 Variation of GHARR-1 power, with the neutron flux (PF) and temperature correlation (PDT) for reactivity released of 4.0 mk at very low power transient

CHAPTER 5

DISCUSSIONS

5.1. Linearity of the MCA used for measurements

Energy calibration performed on the MCA in the gamma spectrometry system for flux measurement was to ensure a qualitative analysis. Fig. 4.1 shows a linear or proportional relationship in a form E=A (CH) + B, where CH is the channel number. It shows that the ^{197}Au spectrum was detected at the exact channel without any offset or pulse pile-up.

5.2. Charge –Sensitivity Pre-amplifier testing

The charge-sensitivity pre-amplifier attached to the HPGe detector was tested with a rectangular input pulse for undershoot which could degrade the energy measurements. It was found to be perfect with the pulse tail decaying along the reference line without undershoot or noise.

5.3. Reactivity of the reactor core at critical neutron flux

It was observed that the neutron flux population in the irradiation site of the reactor core depends on the reactivity level which could be determined by operating the reactor at a critical power of 30 W corresponding to 1.0 x10^9 n/cm^2s (figure. 4.4). Neutron flux reading on the meters of the control systems could not be used to access the flux at a particular power level unless the state of the core is determined. This could also affect activation analysis of samples where the neutron flux value on the meter is used for quantification. At the same time, some element in a particular sample could not show up for lack of enough flux for activation.

5.4. Calculation of neutronics and thermal-hydraulics parameters against Power by semi-empirical relationship

Using the semi-empirical relationship between the reactor power, flux parameters, core inlet temperature and the coolant temperature was observed show that the neutronics power from the flux monitor trailed behind the thermal power due to coolant temperature rise (figure. 4.18). The power due to the flux monitor decreased steadily as the rated power increases. The decrease is as a result of temperature due to nuclear fission which causes the neutron flux to leak out into the coolant. The semi-empirical relation predicted the actual neutronics and thermal powers as pertained in the reactor. Flux readings on the meters of the control systems could not be used to predict the neutronics power unless the reactivity of the core is more than 3 mk. The excess reactivity of GHARR-1 is limited between 3.5 mk and 4.5 mk. The thermal power due to coolant temperature rise could be predicted only when the inlet and outlet temperature probes read correctly.

5.5. Current micro-amplifier calibration

To ensure that the two micro amplifiers in the control systems work perfectly, a current pulse source was used to inject 10 μA in each circuit. The CC and the MCCLS registered 5.03 x 10^{11} and 6.07 x 10^{11} n/cm^{2}s on their respective meters. Using eq.2.1, it was realized that a sensitivity coefficient of 5.0 x 10^4 and 6.0 x10^4 respectively were adopted for the CC and MCCLS and a correction factor of 1.2 employed to obtain a perfect agreement in neutron flux reading (figure. 4.3).

Neutron flux measurements by the two control systems at the same power levels at steady state were the same but at different rod positions. The neutron flux is used by Eq.3.7 to predict the neutronics power of the reactor. The neutronics power obtained

from the meter readings in this work does not reflect the actual power in the inner irradiation sites of the reactor.

5.6. Assessment of negative temperature coefficient reactivity of the reactor

The difference between the inlet and outlet temperatures equals the change in temperature across the core. A fairly constant reactor power with coolant temperature rise was observed. The coolant temperature difference ΔT recorded during operations at different power level and especially at 15 kW was found to be fairly constant with power. However, the control rod position rises gradually with time to compensate for the large negative temperature coefficient of reactivity in order to keep the reactor at the preset power level. This finding satisfies one of the safety requirements of the reactor, which does not permit unnecessary power excursion and the occurrence of boiling.

5.7. The inherent safety of the reactor

It was also observed that at transient state, the correlation between neutron flux and power, as well as temperature and power produced almost the same thermal power at about 20% above the rating power of 30 kW but deviate at lower power. The power decreased gradually from a peak due to temperature effect and accumulation of xenon poison of the core. This demonstrates the inherent safety characteristics of the reactor. Temperature across the core, ΔT was found to be directly proportional to the thermal power, P irrespective of the inlet temperature readings.

5.8. Variation in neutron flux measurements between flux monitor and Console meter readings

The results show that when reactor is operated at different power levels the preset neutron fluxes at the control systems is 1.6 times the neutron fluxes obtained using a flux monitor at the inner irradiation site 2 of the reactor (site 2 generally records maximum flux). The average percentage of deviation of fluxes from the actual preset was 36.5% which compares very well with decrease in core reactivity of 36.3% after operating the reactor at critical neutron flux of 1.0 x 10^9n/cm^{2}s.

5.9. Adjustment of four reactivity regulators

The operating institute of the reactor facility realizing the reactivity level of the core, adjusted the four reactivity regulators upwards to increase the core reactivity to 4 mk. Au-Al wire was used before and after the adjustment of reactivity at a power level of 15 kW to complement the first readings. Neutron flux obtained before and after the adjustment at irradiation site two were 3.20 x 10^{11} n/cm^{2}s and 4.68 x 10^{11} n/cm^{2}s respectively.

5.10. Rectification of inlet temperature readings of the two consoles

The research work led to solving an inlet temperature problem on MCCLS. There was a temperature difference of 4 ^{o}C between the CC and MCCLS at the start of the reactor. This should not have been the case after shutting the reactor down for 64 hours. This led to the replacement of an integrated circuit (IC) U10D and re-soldering of the sensor TMP_{36}. The readings of the two meters of inlet temperatures were now in perfect agreement.

5.11. Reduction in temperature across the core after the upgrade

A steady rise in inlet and outlet temperature with increase in thermal neutrons due to fission was observed. This is due to the compact nature of the core which was designed to cause insufficient thermal circulation of coolant in the core.

It was observed that, operating the reactor at 5.0 x 10^{11}n/cm^{2}s corresponding to 15 kW before the upgrade of the MCCLS in 2008, the coolant temperature difference ΔT recorded during operation ranges between(12.5 -13.5). From 2009 to date, readings ranges between (9.5-11) for both the CC and the MCCLS.

CHAPTER 6

CONCLUSIONS AND RECOMMENDATIONS

6.1. Conclusions

The assessment of the reliability of thermal-hydraulic and neutronics parameters of Ghana MNSR facility for control systems has been investigated at six power levels and at shutdown using GHARR-1. The results obtained show that the neutronics parameters registered on the meters of the control systems at preset thermal neutron flux value cannot be used to estimate the neutron population in the irradiation site of the reactor core. It is always prudent to determine the state of the reactor core. The neutronics parameters could be used to predict the operating power only if the reactivity of the reactor core is between 3.5 - 4.0 mk. When the critical position of the control rod is 112 mm according to the excess reactivity against critical rod position curve, the cold clean core excess reactivity is 3.0 mk and when the rod position increase more than this value reactivity adjustment will be needed using Be plate.

After the installation of the new MCCLS, it was observed that the thermal-hydraulic parameters, especially the coolant temperature difference reduced in value on both controlled systems (CC and MCCLS). The reduction may be due to ageing of the beryllium annular reflector which affected its shape hence allowing more circulation in the core instead of controlled circulation. It could also be attributed to change in the inlet and outlet orifice due to the removal and fixing of the aluminium tray during beryllium addition.

Data obtained in the research work based on the assessment of the reliability of the neutronics and thermal-hydraulic parameters of the control systems of GHARR-1

revealed that an increase in neutron fission (neutron flux) gives a corresponding increase in coolant temperature difference across the core of the reactor.

At a preset neutron fluxes for power levels from shut down to 30 kW, same neutron fluxes were registered but at different control rod positions for the two control systems.

The experimental flux monitor (^{197}Au solution) transferred into the inner irradiation site 2 (where maximum flux is registered) of the reactor core for 23 hrs at shut down measured 1.18 x 10^{6} n/cm^{2}s corresponding to neutronics power of 35 x 10^{-3} W. This is the residual neutron flux in the core at shut down which starts up the reactor without the application of a neutron source. This is at the core reactivity of 2.55 mk.

The trailing of the flux monitor values behind neutron flux read on the meters is due to the decrease of the core excess reactivity from 4.0 mk to 2.55 mk. The excess reactivity of GHARR-1 is limited between 3.5 mk and 4.0 mk in which the instrumentation and control systems work perfectly according to its settings.

It was observed that the step experiment of 2.1 mk reactivity insertion in the reactor core gave rise to a temperature difference across the core from 0.2 to 21.6 ^{o}C and neutron flux from 3.98 x 10^{9} to 1.23 x 10^{12} n/cm^{2}s. The correlation between neutron flux and power, as well as temperature and power at transient state produced almost the same thermal power at about 20% above the rating power of 30 kW. The power (neutron flux) and the temperature began to decrease gradually at 36 kW, which is 20% of the nominal power due to temperature effect and accumulation of xenon poison of the core. This demonstrates the inherent safety characteristics of the reactor. The effect was not experienced at low power.

The research work led to the solving of an inlet temperature problem between the CC and MCCLS by replacing an integrated circuit IC U10D and re-soldering of a dry joint of a temperature sensor TMP_{36}. This enables the two control systems to read same temperature values at start up after shutting down the reactor for 64 hours.

6.2. Recommendations

It is recommended to Nuclear Reactors Research Centre (NRRC) that anytime experiment is going to be carried out using GHARR-1 on neutron flux determination, a critical power of 1.0 x 10^9 n/cm^2s corresponding to theoretical power of 30 W be operated at to determine the core excess reactivity of the reactor core.

That the thickness of the upper beryllium (Be) reflector shall be adjusted when the cold core excess reactivity is less than 3.5 mk. Thickness of Be plate be selected based on calculation using the worth curve of GHARR-1 Beryllium Shim Pieces.

That reactor physicist get involve in reactor operation to ensure that the neutronics and thermal-hydraulic parameters are accurate.

It is recommended that further studies be conducted using different flux monitors and at different core excess reactivity levels for further assessment of meter readings of neutronics and thermal-hydraulic parameters. This could help to assess consistently the reliability of neutronics and thermal-hydraulic parameters measured by the meters. Neutron fluxes in all the irradiation sites (inner and outer) are determined at different power levels.

REFERENCES

[1] Nyarko B.J.B, Ampomah-Amoako E., Amponsah-Abu E.O. Ampong A.G., Opata N.S., Abrefa G., Sogbadji R.B.M., Odoi H.C., Birikorang S.A., Debrah S.K. Ageing Management of Ghana Research Reactor -1.NNRI / GAEC, Box LG. 80, Legon -Accra.Ghana. pp.1-5.

[2] Yamoah S., Akaho E.H.K., Nyarko B.J.B., Asamoah M., Ampong A.G., Amponsah-Abu E.O. (2011) Analysis of Thermal – Hydraulic Transients for the Miniature Neutron Source Reactor (MNSR) in Ghana. pp. 737

[3] Gao Jijin, (1993) General Description of Ghana Miniature Neutron Source Reactor. Training Manual. China Institute of Atomic Energy, Beijing, China pp.6-12.

[4] Research Reactor Instrumentation and Control Technology. (1997). IAEA TECDOC-973, IAEA Vienna, p 7-8, 53-55

[5] Amir Z.M., Pinto J.A., Oliveira de Tello C., Fernando S.L. Digital Control Simulation for Nuclear Reactor Neutronic Parameters. pp. 10-12.

[6] Wang Y., Peng C., Gao J., Chen ShuPing, Li Y (1992). Control System for Miniature Neutron Source Reactor. CIAE, MNSR-DC-3. Beijing.

[7] Wang Yongmao, Gao Jijin, Chen Shuping, Li Yulun. (1992). Maintenance Manual for Control System, Brief Introduction of In-core Micro Fission Chamber. China Institute of Atomic Energy. pp.1-2

[8] Wang Yongmao, (1992). MNSR Control and Protection System. CIAE, Beijing. pp. 3-7, 17

[9] Yu Yuan Fa, Zhu Guo Sheng, Xio Pu, Li Yiguo, (2007) Ghana MNSR Computer Control System. User's Manual. China Institute of Atomic Energy, Beijing, China. pp. 1-5

[10] Standard Test Method for Determining Thermal Neutron Reaction and Fluence Rates by Radioactivation Technique,.(2003). Designation E 262 – 03. ASTM International, 100 Barr Harbor Drive, P. O. Box C 700, West Conshohocken, PA 19428-2959, Unite States. pp.1-2, 4-5

[11] Akaho E.H.K., Maakuu, B.T., Anim-Sampong. S., and Dodoo-Amoo, D.N.A. (1995). On –Site Critical and Zero Power Experiments for Start-up of Ghana Research Reactor-1, GAEC Technical Report, GAEC-NNRI-RT-22.

[12] Akaho E.H.K., Nyarko B.J.B., (2002). Characterization of neutron flux spectra in irradiation sites of MNSR reactor using Westcott-formalism for the K_0 neutron activation analysis method. J. Appl.Rad and Isotop. Vol.57. pp. 265-273

[13] Rant J., (1987). Measurements of neutron flux distribution by activation detectors. IAEA inter-regional course on the application of small computers.

[14] Jong H.M., Sun H.K., Yong S.C.,(2002). Assessment of nuclear characteristics of NAA #1 irradiation hole in HANARO research reactor for application of the K_0-NAA methodology. KAERI, 150 Dukjin-dong, Yuseungu, Daejeon 305-353, Korea. pp.566-573

[15] Gordon G., Hemingway J.D. Practical Gamma Ray-Spectrometry, Nuclear Training Service. Department of Physics, University of Liverpool, Liverpool, UK. pp.56-103

[16] Knoll G.F.(2000). Radiation detection and measurement, 3rd edition. John Wiley & Sons, Inc. New York.pp.201-210

[17] Gbadago J.K., (2010). The Distribution of Naturally Occurring Radionuclide from ore processing to the Environment. PhD thesis, NNRI / GAEC, Box LG. 80, Legon -Accra. Ghana. pp.113-114

[18] Akaho E.H.K., Maakuu B.T., Dodoo-Amoo D.N.A. and Anim-Sampong, S. (1999). Steady State Operational Characteristics of Ghana Research Reactor-1, Department of Nuclear Engineering, National Nuclear Research Institute, Ghana Atomic Energy Commission, Ghana. pp. 18

[19] Zhu G. (1993). Absolute neutron flux measurement by gold foil activation Method. MNSR training material. CIAE, Beijing. pp. 5-6

[20] Sogbadji, R. B. M. (2008). Determination of neutron fluxes of the Ghana Research Reactor -1 and the thermal and epithermal neutron reactions cross sections of Arsenic and Gold by Activation method. M.Phil. thesis, School of Nuclear and Allied Sciences, University of Ghana, Accra/Ghana.

[21] Sogbadji, R. B. M., Nyarko, B. J. B., Akaho, E. H. K., Abrefah, R. G., (2011). Determination of Neutron fluxes and spectrum shaping factors in irradiation sites of Ghana's Miniature Neutron Source Reactor (MNSR) by activation method after compensation of loss of excess reactivity, World journal of nuclear science and technology. pp. 50-56

[22] Baidoo, I. K., (2012) Validation of IAEA ko-instrumental neutron activation analysis software using a low power research reactor GHARR- M.Phil. Thesis, University of Ghana, Legon-Accra, Ghana.

[23] Hao L.(1993). Thermal-hydraulics of MNSR. MNSR training material. CIAE. pp. 1-23

[24] Ampomah-Amoako E., Akaho E.H.K., Anim-Sampong S., Nyarko B.J.B. (2009) Transient analysis of Ghana Research Reactor-1 using PARET / ANL thermal-hydraulic code. SNAS, University of Ghana.

[25] Ahmed Y.A., Balogun G.I., Jonah S.A., Funtua I.I. (2008) The Behavior of Reactor Power and Flux Resulting from change in Core-Coolant Temperature for a Miniature Neutron Source Reactor. Reactor Engineering Section, Centre for Energy Research and Training, Ahmadu Bello University, Zaria, Nigeria. pp. 2417-2419.

[26] Gbadago J.K, Addo M.A., Ennison I., Odoi H. C., Boffie J., Boafo E.K , Sogbadji R.B.M., Abrefah, R.G., Ampong A.G., Amponsah-Abu E.O., Ampomah-Amoako E., . Debrah S.K (Rev. 2012). Safety Analysis Report for GHARR-1. Nuclear Research Institute, Ghana Atomic Energy Commission, P.O.Box LG. 80, Legon, Accra, Ghana. pp. 4-5, 33

[27] Odoi H.C, Akaho E.H.K., Nyarko B.J.B., Abrefah R.G., Ampomah-Amoako E., Sogbadji R.B.M., Birikorang S.A., Gbadago J.K., and Matos J.E., Liaw,J. Morman J., Kalimullah, Mo S.C.. (2011) Current Studies of Conversion of Ghana Research Reactor Core to Low Enriched Uranium. National Nuclear Research Institute, Ghana Atomic Energy Commission, Kwabenya, Accra-Ghana and Argonne National Laboratory, Argonne, IL 60439 USA.

[28] Zhang, Y., Gao J., Chen S., Li Y. (1993). The Whole Simulation Heat Transfer Experiment and Calculation. MNSR Training Materials. CIAE, Beijing, China. pp.2-4,11-12

[29] Hainoun, A., Alissa, S.(2005). Full-Scale Modelling of the MNSR Reactor To simulate normal operation, transients and reactivity insertion accidents Natural

circulation conditions using the thermal-hydraulic code ATHLET. Dept. of nuclear engineering, Atomic Energy Commission, Box 6091, Damascus, Syria. pp. 35, 44-51

[30] Akaho E.H.K., Anim Sampong S., Maakuu B.T, Dodoo-Amoo D.N.A. (2000). Dynamic Feedback Characteristics of Ghana Research Reactor-1. pp. 200-208.

[31] Akaho E.H.K., Maakuu B.T.(2002). Simulations of reactivity transient in a MNSR core. Department of nuclear engineering and design, GAEC Box LG. 80, Legon – Accra. Ghana. pp. 1-63

[32] Hisgadget Inc. mastech – Mas345 PC –interface digital multimeter

[33] ORTEC Solid-State Photon Detector. High- Purity Germanium, Coaxial Photon Detector System. GMX40P4, POPTOP Cryostat Configuration. Serial number 47-TN32309A, USA. pp.1-15.

[34] Systron Donner Corperation, Concord Instrument Division, 10 Systron Drive, Concord, California 94518, USA.

[35] Trio-Kenwood Electronic Inc. CS- 2100, 100MHZ, 4-Channel Oscilloscope. Serial number 1060001-20202000, Komagane, Japan.

[36] Keithley Instruments Inc, Test Instrumentation Group, Fourth Printing (1992). Cleveland, Ohio, USA.

[37] Hogentogler & Co; Inc. Acculab ATL-124 electronic Analytical Precision Balance, Acculab Sartorius Group. Weender Landstresse 94-108,37075 Goettingen, Germany.

[38] Tao, H., Gao, J., Chen, S., Li, Y. (1992). Pneumatic Capsule Transfer System. MNSR –DC-5.CIAE, Beijing. China. pp.1-11

[39] Nuclear Electronics Laboratory Manual, (1984). IAEA – TECDOC- 309, IAEA Vienna, pp. 81-82.

[40] Guo, C. (1993). Experiment of adding top beryllium shims for MNSR. MNSR Training material. CIAE, China. pp.1-2, 12

[41] Yu Yuan Fa, Zhu Guo Sheng, Xio Pu, Li Yiguo, (2007). Ghana MNSR Computer Control System, Principle of Control Circuits. China Institute of Atomic Energy, Beijing, China pp 1-6

APPENDICES

APPENDIX 1

Table 1A: Calibration data obtained for MCA in spectrometry system for gamma energy measurements

Energy (keV)	Channel	Isotope
80.42	168	^{133}Ba
276.37	576	"
302.77	631	"
356.51	743	"
384.34	801	"
660.95	1378	^{137}Cs
1173.29	2449	^{60}Co
1331.83	2781	"

Table 1B: Data obtained from Current Amplifier Calibration for the CC and MCCLS using Keithley model 263 calibrator / source

Source Current Using Keithley Instrument (μA)	Meter Reading CC (n/cm^{2}s)	Meter reading MCCLS (n/cm^{2}s)	Correction Factor	Calculated Values (n/cm^{2}s) Using equation [3.1]		Correction Factor
				CC	MCCLS	
1.0E-03	5.40E+07	6.71E+07	1.24	5.00E+07	6.0E+07	1.2
25E-03	1.25E+09	1.50E+09	1.20	1.25E+09	1.5E+09	1.2
3	1.52E+11	1.81E+11	1.19	1.50E+11	1.8E+11	1.2
10	5.03E+11	6.07E+11	1.20	5.00E+11	6.0E+11	1.2
15	7.50E+11	9.13E+11	1.21	7.50E+11	9.0E+11	1.2
20	9.97E+11	1.22E+12	1.22	10.0E+11	1.2E+12	1.2
			Mean=1.20			Mean=1.2

Table 1C: Experimental and calculated values of current pulses from the Keithley instrument in relation to thermal power and neutron flux

Thermal Power (kW)	Neutron Flux (n/cm^2s)	Experimental Current Pulse CC (μA)	Experimental Current Pulse MCCLS (μA)	Calculated Current Pulse (μA) Using equation [3.1]	
				CC	MCCLS
5	1.67E+11	3.15	2.77	3.34	2.78
10	3.33E+11	6.51	5.50	6.66	5.55
15	5.00E+11	9.90	8.25	10.00	8.33
20	6.67E+11	13.27	11.00	13.34	11.10
25	8.33E+11	16.63	13.68	16.66	13.88
30	9.99E+11	19.98	16.45	19.98	16.65

Table 1D: Values of reactor power obtained using the neutron flux and temperature correlation at neutron flux of 1.67 x 10^{11} n/cm^{2}s for the MCCLS

Time (hrs)	Flux x 10^{11} (n/cm^{2}s)	Rod Position (mm)	Inlet Temperature (°C)	Outlet Temperature (°C)	Change in Temperature-ΔT(°C)	Predicted Power (kW)	Thermal Power Using Temp. Correlation (kW)
10:03	1.67	132	35.4	40.1	4.7	5.0	3.8
10:13	1.67	133	37.2	41.4	4.2	5.0	3.3
10:23	1.68	135	37.7	42.3	4.6	5.04	3.77
10:33	1.67	136	38.9	43.1	4.2	5.0	3.33
10:43	1.67	136	39.6	43.9	4.3	5.0	3.47
10:53	1.66	136	40.3	44.7	4.4	4.98	3.61
11:03	1.67	137	40.4	45.1	4.7	5.0	3.99

Table 1E: Values of reactor power obtained using the neutron flux and temperature correlation at neutron flux of 3.33 x 10^{11} n/cm^{2}s for the MCCLS

Time (hrs)	Flux x 10^{11} (n/cm^{2}s)	Rod Position (mm)	Inlet Temperature (°C)	Outlet Temperature (°C)	Change in Temperature -ΔT(°C)	Predicted Power (kW)	Thermal Power using Temp. Correlation (kW)
09:06	3.32	142	35.8	43.3	7.5	9.96	7.77
09:16	3.33	148	37.8	45.5	7.7	9.99	8.21
09:26	3.31	149	38.0	46.0	8.0	9.93	8.72
09:36	3.33	149	39.6	47.5	7.9	9.99	8.66
09:46	3.33	150	40.1	47.8	8.2	9.99	9.19
09:56	3.31	150	41.2	48.9	7.7	9.93	8.42

Table 1F: Values of reactor power obtained using the neutron flux and temperature correlation at neutron flux of 6.67 x 10^{11} n/cm^{2}s for the MCCLS

Time (hrs)	Flux x 10^{11} (n/cm^{2}s)	Rod Position (mm)	Inlet Temperature (°C)	Outlet Temperature (°C)	Change in Temperature -ΔT(°C)	Predicted Power (kW)	Thermal Power using Temp. Correlation (kW)
14:30	6.69	152	40.6	51.6	11.0	20.07	14.32
14:40	6.66	162	43.5	54.4	10.9	19.98	14.32
14:50	6.69	164	43.9	55.6	11.7	20.07	15.94
15:00	6.66	165	44.6	55.8	11.2	19.98	14.96
15:10	6.67	169	44.9	56.4	11.5	20.01	15.59

Table 1G: Values of reactor power obtained using the neutron flux and temperature correlation at neutron flux of 8.33 x 10^{11} n/cm^{2}s for the MCCLS

Time (hrs)	Flux x 10^{11} (n/cm^{2}s)	Rod Position (mm)	Inlet Temperature (°C)	Outlet Temperature (°C)	Change in Temperature -ΔT(°C)	Predicted Power (kW)	Thermal Power using Temp. Correlation (kW)
09:15	8.34	160	36.5	50.1	13.6	25.02	19.27
09:25	8.33	175	39.1	53.2	14.1	24.99	20.63
09:35	8.29	177	41.8	55.7	13.9	24.87	20.43
09:45	8.36	178	43.6	57.5	13.9	25.08	20.57
09:55	8.37	182	45.2	59.0	13.8	25.11	20.45

Table 1H: Values of reactor power obtained using the neutron flux and temperature correlation at neutron flux of 1.0 x 10^{12} n/cm^2s for the MCCLS

Time (hrs)	Flux x 10^{12} (n/cm^2s)	Rod Position (mm)	Inlet Temperature (°C)	Outlet Temperature (°C)	Change in Temperature-ΔT(°C)	Predicted Power (kW)	Thermal Power Using Temp. Correlation (kW)
09:58	0.997	165	39.4	54.6	15.2	29.91	23.12
10:03	1.00	170	41.0	55.8	14.8	30.00	22.38
10:08	1.00	175	42.8	57.9	15.1	30.00	23.23
10:13	0.997	178	43.4	58.6	15.2	29.91	23.48
10:18	0.997	180	44.3	59.3	15.0	29.91	23.09
10:23	0.998	182	44.9	59.8	14.9	29.94	22.90
10:28	1.00	185	46.4	60.8	14.4	30.00	21.87
						Mean = 29.95	**Mean = 22.86**

Table 1I: Readings before reactivity adjustment at 15 kW

Time (min)	Preset Neutron Flux (n/cm^2s)	Meter Reading (n/cm^2s)	Flux Monitor Au-Al Wire ($n/cm^2 s$)	Ctrl Rod Position (mm)	Inlet Temp. (°C)	Outlet Temp. (°C)	ΔT (oC)
09:06	5.00×10^{11}	5.00×10^{11}	3.20×10^{11}	145	36.0	46.0	10
09:36	"	4.99×10^{11}	"	150	38.7	48.2	9.5
10:06	"	5.00×10^{11}	"	155	41.2	50.6	9.4
10:36	"	5.01×10^{11}	"	157	44.5	54.3	9.8
11:06	"	4.99×10^{11}	"	160	46.0	55.9	9.9
11:36	"	4.98×10^{11}	"	162	46.1	56.1	10
12:06	"	5.01×10^{11}	"	165	46.6	56.8	10.2

Table 1 J: Readings after reactivity adjustment at 15 kW

Time (min)	Preset Neutron Flux ($n/cm^2 s$)	Meter Reading ($n/cm^2 s$)	Flux Monitor Au-Al Wire ($n/cm^2 s$)	Ctrl Rod Position (mm)	Inlet Temp. (°C)	Outlet Temp. (°C)	ΔT (oC)
10:15	5.00×10^{11}	5.01×10^{11}	4.68×10^{11}	129	34.1	43.3	9.2
10:45	"	5.00×10^{11}	"	134	38.0	48.6	10.6
11:15	"	5.01×10^{11}	"	137	40.2	49.8	9.6
11:45	"	5.02×10^{11}	"	140	41.7	51.6	9.9
12:15	"	5.00×10^{11}	"	141	41.9	52.7	10.8
12:45	"	5.00×10^{11}	"	142	42.0	53.0	11
13:15	"	5.02×10^{11}	"	143	44.0	54.1	10.1

APPENDIX 2

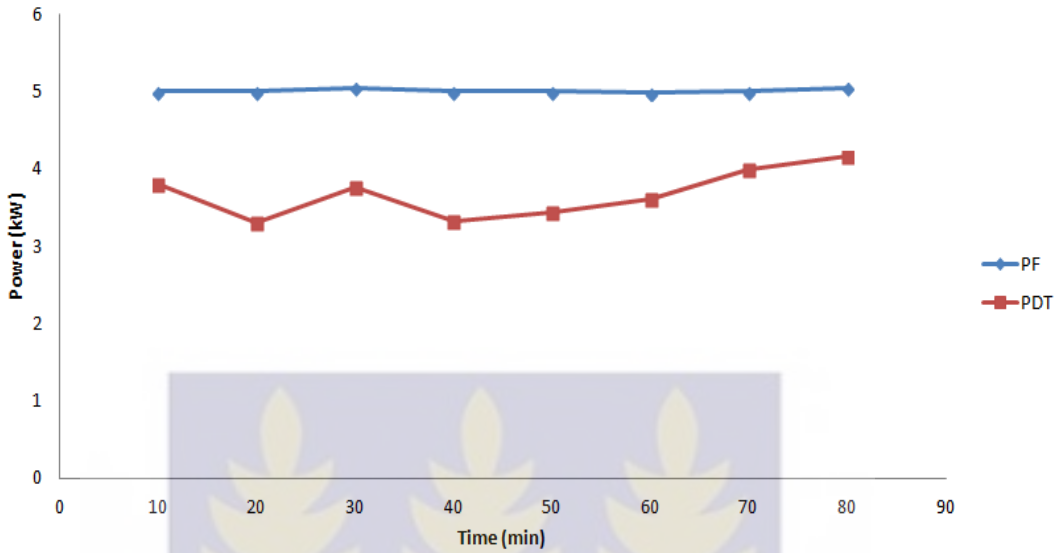

Figure.2A Variation of GHARR-1 neutronics power (P_F) and temperature (P_{DT}) correlation with time for 1.67 x 10^{11} n/cm^{2}s corresponding to 5 kW at steady state

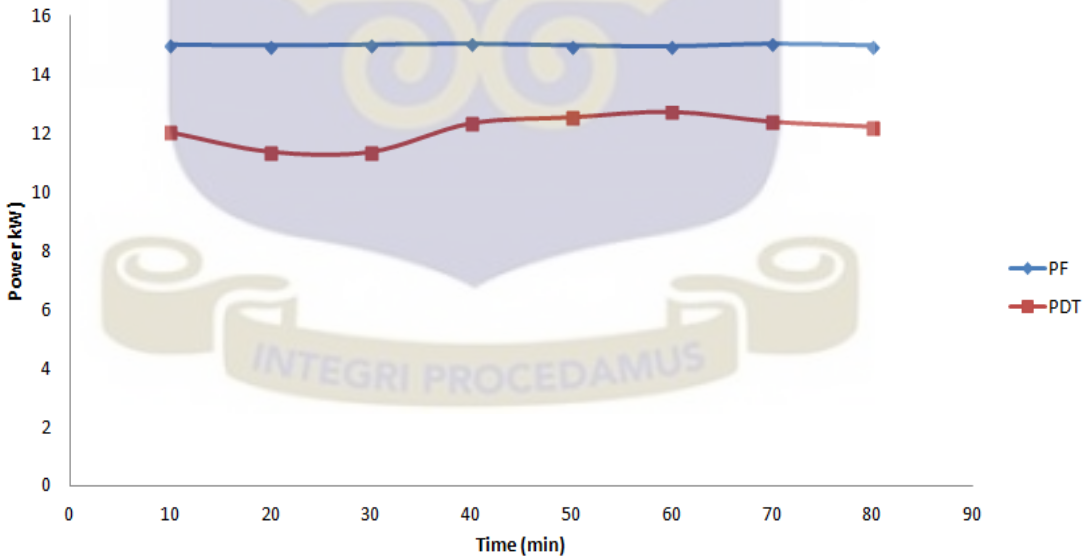

Fig.2B Variation of GHARR-1 neutronics power (P_F) and temperature (P_{DT}) correlation with time for 5.0 x 10^{11} n/cm^{2}s corresponding to 15 kW at steady state

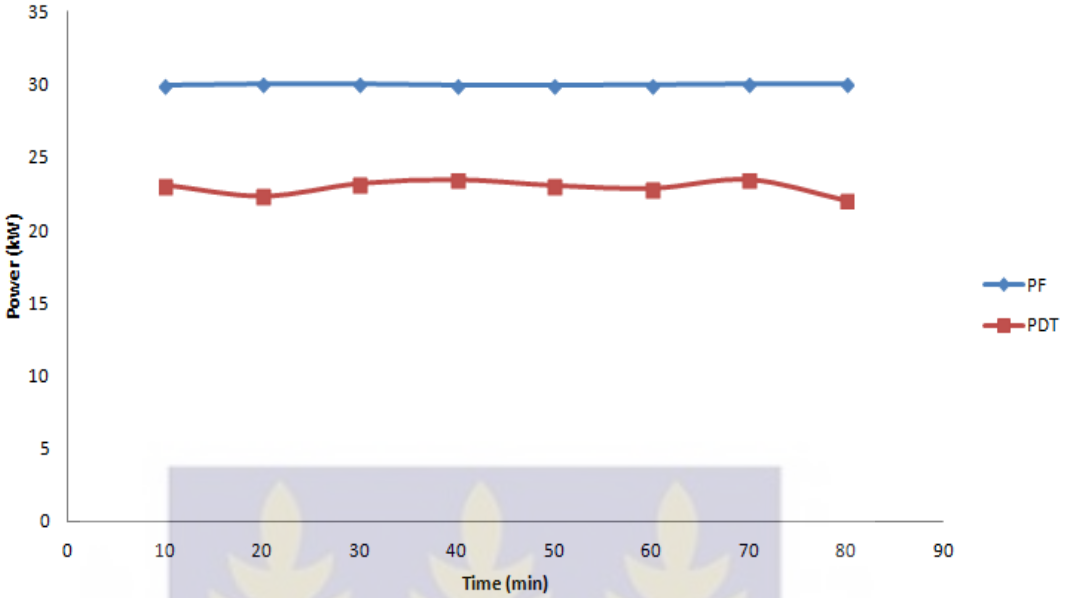

Fig.2C Variation of GHARR-1 neutronics power (P_F) and temperature (P_{DT}) correlation with time for 1.0 x 10^{12} n/cm^{2}s corresponding to 30 kW at steady state

APPENDIX 3

Table 3A: Inlet temperature values measured after the replacement of IC (LM 837) and re-soldering of temperature sensor TMP_{36} for MCCLS at 5.0 x 10^{11} (n/cm^{2}s)

Time (hrs)	Flux x 10^{11} (n/cm^{2}s)	Rod Position (mm)	Inlet Temperature (°C)	Outlet Temperature (°C)
10:5	4.98	145	32.2	32.2
10:35	5.00	149	35.1	45.2
11:05	5.00	152	37.4	47.3
11:35	4.99	155	38.3	47.8
12:05	4.99	156	39.0	49.1
12:35	5.00	158	39.6	49.4
13:05	4.99	160	40.1	49.6

Table 3B: Data for the released of reactivity of 2.1 mk at transient state

Time (Sec)	Log Flux	T_{in} (°C)	T_{out} (°C)	ΔT (°C)	Neutron Flux (kW)	Neutron Power (kW)	Thermal Power (kW)	Difference in Power (kW)	Average Diff. In Power(kW
342	9.6	29.8	30.0	0.2	3.98E+09	0.119	0.027	0.092	
384	9.6	29.8	30.0	0.2	3.98E+09	0.119	0.027	0.092	
486	9.6	29.9	30.1	0.2	3.98E+09	0.119	0.027	0.092	
519	9.61	29.9	30.1	0.2	4.07E+09	0.122	0.027	0.095	
545	9.61	29.9	30.1	0.2	4.07E+09	0.122	0.027	0.095	
578	9.61	29.9	30.1	0.2	4.07E+09	0.122	0.027	0.095	
588	9.69	30.0	30.2	0.2	4.09E+09	0.147	0.027	0.12	
598	9.89	30.0	30.2	0.2	7.76E+09	0.233	0.027	0.206	
611	10.13	30.0	30.2	0.2	1.35E+10	0.405	0.027	0.378	
621	10.40	30.0	30.2	0.2	2.51E+10	0.753	0.027	0.726	
634	10.62	30.0	30.2	0.2	4.17E+10	1.25	0.027	1.223	1.2
647	10.81	30.0	31.1	1.1	6.46E+10	1.94	0.376	1.564	
663	11.06	30.0	32.3	2.3	1.15E+11	3.45	0.701	2.749	
679	11.21	30.0	33.5	3.5	1.62E+11	4.86	2.25	2.61	
699	11.43	30.0	36.4	6.4	2.69E+11	8.07	5.72	2.35	
722	11.61	30.0	38.5	8.5	4.07E+11	12.2	8.85	3.35	
748	11.74	30.0	42.3	12.3	5.50E+11	16.50	14.8	1.70	
774	11.85	30.0	44.1	14.1	7.08E+11	21.24	19.4	1.84	
800	11.94	30.0	45.9	15.9	8.71E+11	26.13	23.3	2.83	
833	12.02	30.0	48.6	18.6	1.05E+12	31.50	28.7	2.8	
866	12.05	30.0	50.1	20.1	1.12E+12	33.60	33.5	0.1	
902	12.07	30.0	50.4	20.4	1.17E+12	35.00	34.5	0.5	
916	12.07	30.1	51.1	21.0	1.17E+12	35.10	35.9	-0.8	
930	12.07	30.1	51.1	21.0	1.17E+12	35.10	35.9	-0.8	
953	12.07	30.7	51.7	21.0	1.17E+12	35.10	36.4	-1.3	
979	12.09	31.1	52.3	21.2	1.23E+12	36.90	37.0	-0.1	0.7
1010	12.09	31.1	52.4	21.3	1.23E+12	36.90	37.0	-0.1	
1030	12.09	31.2	52.7	21.5	1.23E+12	36.90	37.58	-0.68	
1130	12.09	32.2	53.7	21.5	1.23E+12	36.90	37.7	-0.8	
1330	12.09	32.2	53.8	21.6	1.23E+12	36.90	37.77	-0.87	
1510	12.08	33.4	53.5	20.1	1.20E+12	36.00	37.2	-1.2	
1710	12.02	34.3	53.5	19.2	1.05E+11	31.50	32.14	-0.64	

Table 3C: Data for the released of reactivity of 4.0 mk at transient state

Time (Sec)	Log Flux	Tin (°C)	Tout (°C)	ΔT (°C)	Neutron Flux (kW)	Neutron Power (kW)	Thermal Power (kW)	Difference In Power (kW)	Average Diff. In Power(kW)
112	7.49	29.2	29.5	0.3	3.09E+07	0.001	0.049	-0.048	
130	7.53	29.2	29.5	0.3	3.39E+07	0.001	0.049	-0.048	
170	7.53	29.2	29.7	0.5	3.39E+07	0.001	0.109	-0.108	
178	7.70	29.2	29.7	0.5	5.01E+07	0.002	0.109	-0.107	0.07
185	8.09	29.2	29.7	0.5	1.23E+08	0.004	0.109	-0.105	
191	8.43	29.2	29.7	0.5	2.69E+08	0.008	0.109	-0.101	
197	9.13	29.2	29.7	0.5	1.35E+09	0.041	0.109	-0.068	
202	9.52	29.2	29.8	0.6	3.31E+09	0.099	0.144	-0.045	
206	9.84	29.2	29.8	0.6	6.92E+09	0.208	0.144	0.064	
210	10.2	29.0	29.8	0.8	1.58E+10	0.474	0.225	0.249	
213	10.6	29.0	29.8	0.8	3.98E+10	1.19	0.225	0.956	
219	10.9	29.0	29.8	0.8	7.94E+10	2.38	0.225	2.155	
223	11.3	29.0	29.8	0.8	1.99E+11	5.97	0.225	5.745	13.2
229	11.7	29.0	29.9	0.9	5.01E+11	15.0	0.269	14.731	
237	12.0	29.0	31.2	2.2	1.0E+12	30.0	1.078	28.92	
248	12.16	29.0	37.0	4.4	1.44E+12	43.2	3.16	40.04	
261	12.25	29.0	48.8	15.9	1.77E+12	53.1	23.12	29.98	
276	12.3	29.0	59.0	30.0	1.99E+12	59.7	61.89	-2.19	
293	12.35	29.0	63.5	34.2	2.24E+12	67.2	75.8	-8.6	
311	12.38	29.0	67.1	38.1	2.39E+12	71.7	89.7	-18.0	
349	12.44	29.0	71.7	42.7	2.75E+12	82.5	107.0	-24.5	
367	12.46	29.0	72.3	43.3	2.88E+12	86.4	109.4	-23.0	
446	12.47	31.7	74.8	43.1	2.95E+12	88.5	109.7	-21.2	17
547	12.48	33.1	75.4	42.3	3.02E+12	90.6	107.2	-16.6	
639	12.49	351	75.6	40.5	3.09E+12	92.7	100.6	-7.9	
719	12.49	36.2	76.1	40.4	3.09E+12	92.7	98.9	-6.2	
752	12.45	36.8	76.3	39.5	2.82E+12	85.6	97.1	-11.5	
837	12.38	37.9	76.2	38.3	2.40E+12	72.0	93.0	-21	
848	12.21	37.6	75.9	38.3	1.62E+12	48.6	92.7	-44.1	